UNIVERSIDADE DE LISBOA
FACULDADE DE CIÊNCIAS
DEPARTAMENTO BIOLOGIA VEGETAL

Vectored immunoprophylaxis to produce anti-BACE1 nanobodies for treatment of Alzheimer's disease

Maria Eugénia Freire Torres Alves Machado

Mestrado em Biologia Molecular e Genética

Dissertação orientada por:
Prof. Dr. Matthew Holt
Prof. Dr. Cláudio M. Gomes

2019

Acknowledgments

To the Matthew Holt group
I am truly thankful for the opportunity that was given to me, it was a very challenging and enriching experience. I want to thank Marika Marino for her friendship and counselling, for patiently listening to my questions and condone with my weird self, but above all for her motivation, trust, and constant care. I want to thank Dr. Melvin Rincon for his supervision, shared knowledge and for believing in me. I grew as a person and as a scientist thanks to this experience and to the people with whom I worked alongside.

To Faculdade de Ciências da Universidade de Lisboa
I want to thank Professor Cláudio Gomes, for the supervision he provided, for his advices and support.

To all my friends and family
I want to thank my family, as I wouldn't be where I am today without their constant support. For the friends that motivate me, inspire me and are present in each and every single step of my life. I want to thank Margarida Godinho, Carolina Saraiva, João Zagalo, André Barateiro, João Santos, Rafael Luís, David Santos, Sofia Andrêzo, Diana Coito.
To the my portuguese friends that I met in Leuven, you made a foreign country feel like home, I wouldn't want to share those moments with anyone else.

The work presented in this thesis was developed from september 2018 to july 2019 at the Matthew Holt Lab at the VIB-KU Leuven Center for Brain & Disease Research, Belgium, in the framework of an ERASMUS+ internship.

Table of contents

List of abbreviations

AAV	Adeno-associated virus
Aβ	Amyloid-β
AD	Alzheimer's disease
Ad	Adenovirus
AICD	Amyloid precursor protein intracellular domain
APP	Amyloid precursor protein
BACE	β-site amyloid precursor protein cleaving enzyme
BBB	Blood-brain-barrier
BSA	Bovine serum albumin
CAA	Cerebral amyloid angiopathy
CBA	Cytomegalovirus/chicken β-actin
CHAPS	3-[(3-Cholamidopropyl) dimethylammonio]-1-propanesulfonate
CIP	Calf Intestinal Phosphatase
CNS	Central nervous system
CREATE	CRE-recombination based AAV target evolution method
DOC	Deoxycholate
FAD	Familial Alzheimer's disease
HIV	Human immunodeficiency viruses
HSV	Herpes Simplex Virus
IP	Intra-peritoneally
ITR	Inverted terminal repeats
LB	Lysogeny broth
LC-MS/MS	Liquid chromatography coupled to mass-spectometry in tandem
LV	Lentivirus
mRNA	Messenger RBA
mAb	Monoclonal antibody
NFT	Neurofibrillary tangles
NMDA	N-methyl-D-aspartate
ORF	Open reading frame
pA	Poly-A
PBS	Phosphate buffered saline
PI	Phosphatase inhibitor
PSEN	Presenilin
sc	Self-complementary
scFV	Single-chain variable fragments
SOC	Super optimal broth with catabolite
ss	Single-stranded
TB	Terrific broth
TBS	Tris buffered saline
TMB	Tetramethylbenzidine
T-PER	Tissue protein extraction reagent
TREM	Receptor expressed on myeloid cells 2
vg	Vector genome
VIP	Vectored immunoprophylaxis
WPRE	Woodchuck post-trasnscriptional regulatory element

List of tables

List of figures

Abstract

Alzheimer's disease (AD) is the main cause of dementia, a disease characterized by an impairment in memory, language, and cognition. It is estimated to affect around 46 million people worldwide. The economic costs of AD will soon be unbearable. Therefore, efforts to find a treatment to halt or even slow the progression of the disease have become a priority for the scientific community. The symptoms of AD are cognitive impairment and progressive neurodegeneration. At the cellular level, the abnormal deposition of amyloid-β (Aβ) species is thought to be the trigger of the disease, although there are cellular stressors that also play a role in the progression of AD. β-site amyloid precursor protein cleaving enzyme 1 (BACE1) is responsible for 80% of Aβ production in the brain. Hence, strategies such as small molecules inhibitors or antibodies targeting BACE1 have been generated. However, limitations such as cross-reactivity with BACE2 and poor blood-brain-barrier (BBB) crossing respectively, have limited their success. In this context, gene therapy has emerged as an alternative approach for the treatment of neurodegenerative diseases like AD. Therapies for central nervous system (CNS) based on the use of adeno-associated virus (AAV) are being widely developed, as they have the advantages of providing a higher specificity to the target, being safe, infect several cells types and provide long-term expression of any given therapeutic transgene. Thus, strategies such as passive immunization by AAV-mediated delivery of antibody-encoding genes (vectored immunoprophylaxis: VIP) may be an ideal alternative to treat not only AD, but also a wide spectrum of neurodegenerative disorders. Here, a novel AAV-based therapeutic strategy is evaluated, aiming to deliver an anti-BACE1 nanobody that efficiently decreases the levels of Aβ in the CNS after systemic delivery. Therefore, we validated the expression of the nanobody in three AD mouse strains: APP^{Dutch}, APP^{NL-G-F} and APP/PS1. The activity of the nanobody was evaluated indirectly by measuring Aβ content in tissue extracts. A significant reduction in Aβ was observed in APP^{Dutch} and APP^{NL-G-F}. However, the Aβ content did not change in the APP/PS1 strain, most probably due to the severity of amyloidosis, characteristic of this model. In this thesis, we attempted an optimization of the AAV vector to boost the nanobody transgene expression by using a self-complementary (sc) AAV conformation.

Keywords: AAV vector, gene therapy, Alzheimer's disease, vectored immunoprophylaxis, nanobody

Resumo

Atualmente, a Doença de Alzheimer é a principal causa de demência, afetando mundialmente cerca de 46 milhões de pessoas. A incessante procura de uma cura para o Alzheimer, de terapias que impeçam a propagação da doença ou até mesmo de biomarcadores para o diagnóstico prematuro da doença, está longe de acabar. No entanto, os custos relacionados com esta doença serão incomportáveis nas próximas gerações. Em 1906, Alois Alzheimer descreveu pela primeira vez uma doença que numa fase celular foi caracterizada pela formação de emaranhados neurofibrilhares e pela deposição de placas amilóides no cérebro, posteriormente ocorre perda neuronal, distrofia dos astrócitos e neurónios e alterações vasculares, nesta fase, os pacientes apresentam declínio cognitivo e por fim demência. A maioria dos casos de Alzheimer são esporádicos e surgem em pacientes com idade avançada. No entanto, existem casos hereditários e de *early onset*, que ocorrem devido a mutações em genes que codificam para as presinilinas (PSEN) e para a *amyloid precursor protein* (APP), proteínas que estão envolvidas na via amiloidogénica, e que favorecem a formação das espécies de amilóide-β (Aβ) tóxicas. A hipótese de cascata amiloidogénica propõe que as placas amilóide, os péptidos Aβ que as constituem, e o seu metabolismo, têm um papel fundamental no desenvolvimento da doença de Alzheimer. Consequentemente, mutações nas PSEN e em APP, enzima e substrato da via amiloidogénica, são causadoras da doença, e são frequentemente manipuladas para criar modelos de Alzheimer *in vitro* e *in vivo*. O modelo de cascata amiloidogénica, por ter apenas em conta o papel da deposição das placas amilóides ao nível dos neurónios, exclui outros elementos, como a neuroinflamação e a disrupção da barreira hemato-encefálica (BBB), que também apresentam uma função fundamental no desenvolvimento do Alzheimer.

A enzima BACE1 (*β-site amyloid precursor protein cleaving enzyme* 1) é a responsável pelo processamento da APP pela via amiloidogénica, deste modo, tem sido um dos principais alvos de investigação para terapias de Alzheimer. Inibidores de BACE1 têm sido um êxito em estudos *in vitro,* sendo que muitas moléculas com potencial terâpeutico avançarem para ensaios clínicos, no entanto a maioria dos ensaios não foram bem sucedidos e foram posteriormente descontinuados. Uma alternativa às moléculas inibidoras de BACE1 é, então, a administração de anticorpos anti-BACE1, que por serem mais estáveis e apresentarem uma maior especificidade ao substrato, tem um elevado interesse terâpeutico. No entanto, até estas moléculas apresentam desvantagens, tais como ineficiência em atravessar a BBB e um tempo de vida curto. O desenvolvimento de terapia génica baseada em vetores virais permite o transporte de genes de que codificam para anticorpos, ultrapassando as desvantagens dos anticorpos.

Recentemente, a terapia génica baseada em vetores virais emergiu como um método eficiente de expressão de genes com potencial terâpeutico, através de técnicas moleculares. Este método, dependendo da origem do vetor, tem duas subdivisões. A terapia génica não viral, que consiste na administração de moléculas de origem não viral, tal como polimeros catiónicos, lípidos catiónicos, entre outros. Estes métodos apesar de baratos, não são eficientes para o tratamento de doenças do sistema nervoso central (CNS). Por outro lado existe a terapia génica viral , em que variados tipos de vetores têm sido desenvolvidos, sendo os mais estudados os adenovírus, lentivírus e vírus adeno-associados (AAV), sendo este último mais eficientes. AAV são vírus não replicativos e não patógénicos, que contêm um genoma de 4,7 kb de DNA de cadeia simples. Os vetores AAV não integram o genoma, e são produzidos através da remoção dos genes virais que são flanqueados pelas duas regiões terminais invertidas (ITR), sendo posteriormente substituídos por uma cassete de expressão génica que contém o gene de interesse. Existem 11 serótipos naturais e cerca de 100 variações destes, sendo este determinado pela sequência de amino-ácidos

da cápside, sendo que o tropismo de cada serótipo depende da cápside. O serótipo 9 e o serótipo PHP.B, uma variação do serótipo 9, apresentam uma grande afinidade para células do sistema nervoso, sendo que o último é bastante eficiente a atravessar a BBB e a transduzir células nervosas. O genoma destes vetores pode adquirir duas conformações, uma de cadeia simples (ss), outra de cadeia complementar (sc), a segunda é formada devido a uma mutação em um dos ITR, que confere à molécula de DNA uma conformação de cadeia dupla, pronta a ser transcrita pela maquinaria da célula hospedeira, sendo que ambos permitem uma expressão contínua do transgene. A conformação sc permite uma expressão do transgene mais rápida e mais eficiente, apesar a capacidade de transporte do vetor diminuir para 2,5 kb. O desenvolvimento e otimização destes mecanismos permitem ao vetor atravessar a BBB, eficientemente transduzir neurónios e aumentar a expressão de moléculas terapêuticas, tais como anticorpos ou nanoanticorpos altamentes eficientes. Esta técnica é chamada de *vectored immunoprophylaxis* (VIP).

VIP consiste na imunização passiva de anticorpos através de terapia génica baseada em vírus, sendo que as células transduzidas expressam o anticorpo codificado no transgene, estas proteínas tem uma expressão endógena e continuada, permitindo que apenas uma administração do vetor tenha um efeito prolongado. Os anticorpos monoclonais, apesar de apresentarem resultados positivos, tem-se provado ineficientes após administração de vetores que contêm a sua informação génetica no genoma, contrariamente aos nanoanticorpos. Os nanoanticorpos são produzidos por camelídeos e são pequenas moléculas com alta estabilidade, baixa imugenogeneicidade e alta afinidade para pequenos antigénios. Os nanoanticorpos, devido ao seu tamanho, são facilmente introduzidos no genoma de um vetor scAAV, que apresenta uma conformação que aumenta a expressão do transgene contido no seu genoma.

Este trabalho focou-se no desenvolvimento de uma nova terapia VIP baseada em vírus AAV. O vetor administrado continha no seu genoma o transgene que codifica para um nanoanticorpo com atividade anti-BACE1 (B9), anteriormente validado *in vitro*. Após administração do vetor que continha o gene que codifica para o nanoanticorpo B9, a diminuição do conteúdo Aβ foi detetável em duas das três estirpes em estudo, APP^{Dutch} e $APP^{NL\text{-}G\text{-}F}$, no entanto não foi detetável a alteração nos níveis de Aβ na estirpe APP/PS1, possivelmente devido à agressividade do modelo na deposição das espécies Aβ. A optimização do vetor é fundamental para aumentar a expressão do transgene e para aumentar o efeito terâpeutico do nanoanticorpo de modo a que haja uma diminuição dos niveís de Aβ. Deste modo, avaliou-se a eficiência de um vetor com uma conformação scAAV, sendo expectável que aumente a expressão do transgene. Os conteúdos de Aβ entre os grupos injetados com ssAAV e o scAAV permaneceram semelhantes aos do grupo injetado com o vetor controlo, possivelmente devido à baixa concentração de Aβ nos cérebros dos ratos APP^{Dutch} na idade analisada. Posteriormente, a expressão do nanoanticorpo após injeção com as duas conformações, ssAVV e scAAV, foi comparada. No entanto e contrariamente ao expectável, a conformação ssAAV conferiu uma expressão mais acentuada do que a conformação scAAV, deste modo concluimos que os benefícios que advêm a conformação sc não compensam a perda dos elementos regulatórios presentes no vetor com a conformação ss.

A administração de vetores capazes de transportar um nanoanticorpo com efeitos terapêuticos é de elevado interesse não só para tratamento do Alzheimer mas também para o tratamento de outras doenças do CNS. A administração de B9 por via de um AAV vector, ainda precisa de otimização, no entanto apresenta um grande potencial terapêutico.

Palavras-chave: vetor AAV, terapia génica, doença de Alzheimer, *vectored immunoprophylaxis*, nanoanticorpo

1 Introduction

1.1 Alzheimer's disease

Alois Alzheimer described in 1906 "a peculiar severe disease process of the cerebral cortex", a disease that was later described by the deposition of neuronal tangles and amyloid plaques in the brain, associated with astrocytic and neuronal dystrophy, neuronal loss and vascular alterations (Hippius and Neundörfer, 2003; De Strooper and Karran, 2016). The German psychiatrist described the pathology in the patient August Deter (Jarvik and Greenson, 1987), whose symptoms included progressive memory loss, cognitive and functional impairment, and psychiatric disturbances.

1.1.1 Global Impact of Dementia and Alzheimer's

Nowadays this disease, known as Alzheimer's disease (AD), is the most common cause of dementia. It is estimated that 47 million people worldwide are diagnosed with dementia, representing a socioeconomic burden for society, which will be unbearable in the next generations (Picanco, *et al*., 2018; Prince *et al*., 2016; Saito and Saido, 2018). By 2030, it is estimated that the total cost of this disease will reach 2 trillion USD dollars. By 2050, 68% of dementia cases are expected to occur in low to middle income countries (Prince *et al*., 2015).

AD neuropathology is hypothesized to begin before appearance of mild cognitive impairment and dementia state (Heneka *et al.,* 2015). At the cellular level, an accumulation of extracellular amyloid-β (Aβ) plaques occurs, together with an intracellular accumulation of hyperphosphorylated tau protein, which forms neurofibrillary tangles (NFT) (Sakakibara *et al*., 2018; Braak and Braak, 1991; Hyman *et al*, 2012; Serrano-Pozo *et al.*, 2011). These molecular processes are accompanied by astrocytic and microglial activation (Jankowsky and Zheng, 2017). Amyloid plaques and NFT are considered the pathological hallmarks of AD. They begin to appear in the cortex, 25-30 years (for the plaques) and 15 years (for the NFT) before the symptoms of AD start to appear (Saito and Saido, 2018; Selkoe and Hardy, 2016; Bateman *et al.,* 2012).

Currently, there are no effective therapies for established AD, or even treatments which slow disease progression. There is also a lack of validated biomarkers hampering early diagnosis of AD (Peng *et al.,* 2016; Heppner *et al*, 2015). However, there are therapies available that delay the appearance or the progression of the symptoms, providing symptomatic relief (Wisniewski *et al*., 2012; Kumar *et al*., 2014). In early stages of the disease prevention therapies, such as the administration of the Aβ-specific vaccine CAD106 were unsuccessfully attempted (Karran *et al,* 2011). Moreover, there are also symptomatic therapies such as cholinesterase inhibitors and N-methyl-D-aspartate (NMDA) receptor antagonist-memantine (Ferreira-Vieira *et al*. 2016, Omerovic *et al.*, 2008). The basis for the cholinesterase inhibitors therapies is acting on delaying the breakdown of acetylcholine (Ach) since AD brains show defects in cholinergic transmission. Memantine acts on the excitotoxicity caused by glutamate, which is one of the consequences of AD (Lewerenz and Maher, 2015). Although the current alternatives for AD patients may delay the progression of the symptoms (Omerovic *et al.,* 2008) and provide symptomatic relief, a therapy that halts the progression of the disease at a mechanistic level is still needed.

The majority of AD cases are late onset and sporadic, with no evident Mendelian pattern, with the risk of disease increasing with life expectancy (Heppner *et al.,* 2015; Querfurth and Laferla, 2010). These cases are due to a network of environmental, genetic and lifestyle factors (Lahiri *et al,* 2004). However, there is a small percentage of AD cases with a hereditary pattern caused by specific established mutations, known as familial Alzheimer's disease (FAD) (De Strooper and Karran, 2016). These mutations are present in genes such as presenilin (PSEN1, PSEN2) and amyloid precursor protein (APP), which is a type I transmembrane expressed in the brain. These genes take part in the amyloidogenic pathway, and when mutated, APP is cleaved in a manner that favors formation of Aβ42 (Jankowsky and Zheng, 2017), a toxic species which is known to aggregate and initiate the disease. Mutations in PSEN1 and PSEN2 are the most common mutations identified in FAD (Veugelen *et al.,* 2016). PSEN provides the catalytic core to γ-secretase, which participates in the processing of APP (Veugelen *et al.,* 2016; Matsumura *et al.*, 2014; De Strooper *et al*., 1998; Wolfe *et al*., 1999). Furthermore, there are reports including other genetic risk factors for sporadic forms of AD, such as point mutations in a receptor expressed on myeloid cells 2 (TREM), and the presence of the allele of ApoliproteinE ε4 (Jankowsky and Zheng, 2017).

1.1.2 Amyloid Cascade Hypothesis

The amyloid cascade hypothesis, a neuron-centric model, proposes that amyloid plaques, their constituent Aβ peptides, and disturbances in Aβ metabolism, play a central role in AD (De Strooper and Karran, 2016).

The basis for the amyloid cascade hypothesis lies in the production of Aβ through the cleavage of APP by β- and γ-secretases. There are two pathways of cleavage of APP: the non-amyloidogenic and the amyloidogenic one (Fig. 1). In the non-amyloidogenic pathway, APP is processed by α-secretases and γ-secretases, producing a sAPPα ectodomain, a p3 fragment, and an amyloid precursor protein intracellular domain (AICD). sAPPα is thought to have functions like neurotransmission and synaptic plasticity among others (Wang *et al.,* 2014; Seabrook *et al.*, 1999; Yang *et al*., 2009; Mockett *et al*., 2017; Muller *et al.* 2017). The AICD has a role in regulating transcription (Kimberly *et al*.,2001; Cupers *et al.,* 2001), meanwhile, the p3 fragment is also found in amyloid plaques. The amyloidogenic pathway aforementioned is initiated by activity of the β-secretase and continued by γ-secretases. This pathway produces sAPPβ, AICD and Aβ peptides. Aβ peptides are known to be prone to aggregate and form soluble oligomers, that turn into protofibrils, this species maturse and forms fibrils, which aggregate and deposit in the form of senile plaques (Kumar *et al*., 2015).

The β-site amyloid precursor protein cleaving enzyme 1 (BACE1), a β-secretase, is a type I transmembrane protein that processes the amyloidogenic pathway. BACE1 is an aspartyl protease from the peptidase A1 family (Vassar *et al*.,1999), commonly expressed in the brain, especially in neurons. This enzyme became the main target for AD therapy since it was discovered in 1999 due to its key role in the amyloid cascade hypothesis, since it is responsible for 80% of all Aβ production (Read and Suphioglu, 2013).

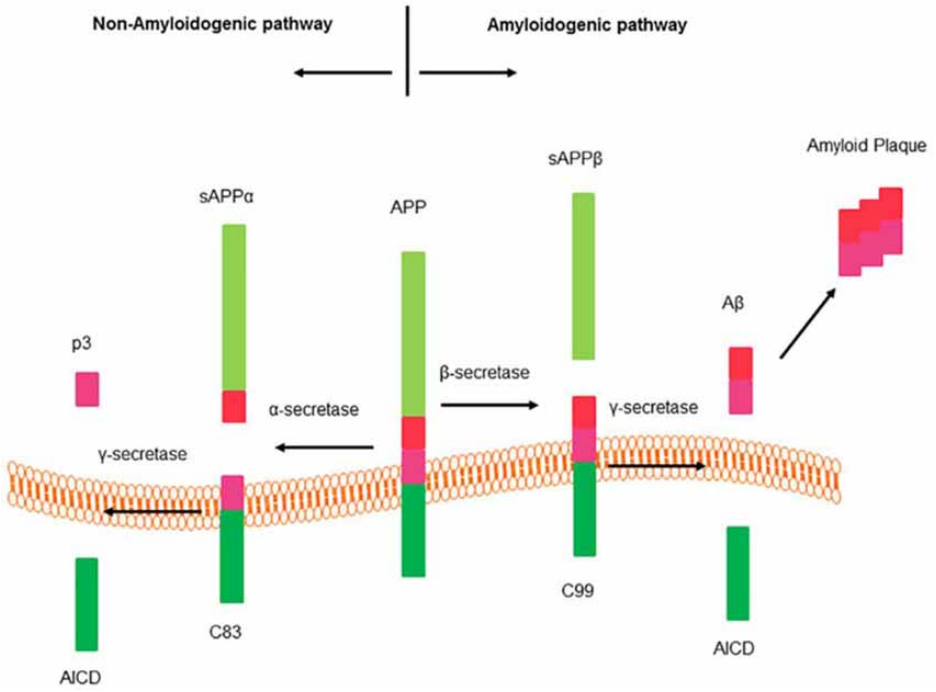

Figure 1. Amyloid precursor protein (APP) processing pathways (Graphic adapted from Zhao *et al.,* 2016)

The Aβ species found in AD and normal brains are disparate. In normal brains, the most abundant species is Aβ40. Meanwhile, in AD brains, Aβ42 and longer species are the most prevalent. This difference is, in part, due to γ-secretases that cleave fragments of different sizes (Portelius *et al.,* 2010; Chavez-Gutierrez *et al*., 2012). Moreover, Aβ42 oligomers are responsible for inducing oxidative stress and tau hyperphosphorylation, which cause toxic effects and neuronal degeneration (Kumar *et al.,* 2015).

However, this model lacks the inclusion of the role of other cellular players, does not take into account interactions between the different cell types, and the progression of the disease, nor does it explain the asymptomatic period of AD (De Strooper and Karran, 2016). The amyloid cascade hypothesis, being a quantitative model (higher concentration of Aβ, means higher concentration of plaques, and consequently progression of AD), does not provide an explanation for the qualitative aspects. For instances, mutations in PSEN cause a disruption in the cleavage of Aβ, generating species longer than Aβ40, which are more prone to aggregate and deposit in plaques (De Strooper and Karran, 2016; Chavez-Gutierrez *et al.*, 2012; Szaruga *et al.,* 2015; Saito *et al*., 2011).

1.1.3 AD-Related Stressors

Additional stressors involved in AD development include neuroinflammation, vascular modifications among others (De Strooper and Karran, 2016). Neuroinflammation is a protective mechanism, mediated by microglia, astrocytes, neurons, T-cells and other mediators (Kempuraj

et al., 2017). Initial inflammatory responses are thought to preserve homeostasis in the central nervous system (CNS), partially restoring the damaged glial cells and neurons. Once the responses become chronic and inhibit the neuronal regeneration, inflammation favors disease progression independently from the deposition of the plaques and the NFT, becoming irreversible and pathological (De Strooper and Karran, 2016; Kempuraj *et al*., 2017).

The integrity of the blood-brain barrier (BBB) also plays an important function, due to its role in the clearance of Aβ (De Strooper and Karran, 2016). The BBB is constituted by astroglial end-feet, endothelial cells and pericytes and smooth muscle cells. Gap junctions in the BBB allow the passage and elimination of Aβ and tau. Defects in this mechanism may lead to neuroinflammation, vascular and synaptic dysfunction, which may lead to the progression of AD (De Strooper and Karran, 2016).

1.1.4 BACE1 as a potential therapeutic target for AD

According to the amyloid cascade hypothesis, lowering levels of Aβ levels would be sufficient to halt the progression of the disease, although a complicating factor may be the differences in propensity to aggregate between Aβ species (De Strooper and Karran, 2016). The findings that BACE1 acts on the first and rate-limiting step in Aβ generation in the brain, and that the loss of β-secretase activity in knock-out mouse models showed a reduction in β-amyloid peptide production, clearly indicate that BACE1 is an excellent therapeutic target for the treatment of AD (Luo *et al.*, 2001; Roberds *et al*., 2001). The defects shown in the knock-out mice were mainly related to BACE1 inhibition during developmental stages and are due to other substrates of BACE1 and not APP (Barão et al, 2016), meaning that the current therapies should be safe since they are administered in adults (Roberds *et al*., 2001). There are small molecules used for inhibition of BACE1 that reached phase 2/3 clinical trials, which are shown to be safe, but overall, they were ineffective and were discontinued, possibly due to some factors, such as solubility, bioavailability, and potency among others (Read and Suphioglu, 2013). For instances, the promising Merck's Verubecestat administered to patients with mild-to-moderate AD was discontinued in 2017 due to "virtually no chance of finding a positive clinical effect (Hawkes, 2017). In July 2019, the Amgen/Novartis' Umibecestat (CNP520) was also discontinued due to worsening of the symptoms. In September 2019, the promising Eisei/Biogen's Elenbecestat was also discontinued, due to a finding of unfavorable risk/benefit (NCT02956486).

Additionally, some BACE1 inhibitors show an additional problem, cross-reactivity with BACE2, also a β-secretase with around 49% homology with BACE1. Although BACE2 is expressed mainly in colon, kidneys, and pancreas (Yan *et al*., 2017; Read and Suphioglu, 2013), this cross-reactivity could increase the risk of off-target toxicity. For instances, BACE2 also processes the pigment cell-specific melanocyte protein, that is one of the responsible proteins for the formation of the melanosome complex in pigment cells (Rochin *et al.,* 2013). Hence, BACE 2 inhibition results in hypopigmentation, which indeed is the most consistent phenotype in pre-clinical studies where BACE1/2 are inhibited, a clear sign of cross-reactivity (Dominguez *et al.,* 2005; Shimshek *et al.,* 2016). Unfortunately, most of the compounds that reached a clinical trial level have shown some degree of cross-reactivity (Farzan *et al.*, 2000; Shimshek *et al.*, 2016).

An alternative to small molecules inhibitors is the administration of antibody-based therapies. Antibodies are more stable and more target specific compared to the BACE1 inhibitors in study. However, these molecules also present some drawbacks, for instances after systemically delivery

of the antibody, only a small fraction of it crosses the BBB. Moreover, a direct intracerebral injection of an anti-BACE1 antibody proved to be efficient in the hippocampus of APP^{Dutch} mice, although this invasive strategy is not ideal for translational purposes. (Zhou *et al.*, 2011). Many strategies were developed to surpass this limitation, such as ultrasonic opening of the BBB, among others (Jordão *et al.,* 2010), however they all showed perturbation of brain homeostasis and low efficiency. Currently, gene therapy using viral vectors is being to deliver transgenes that encode therapeutic proteins, such as anti-BACE1 antibodies.

1.2 Gene therapy as therapeutic approach for CNS diseases

Gene therapy has become a hot topic in the past few years. The Human Genome Project and the identification of genes underlaying Mendelian disorders created the concept that DNA can be manipulated as a clinical therapy (Kotterman *et al.*, 2015; Rommens *et al.*, 1989; Riordan *et al.*, 1989; Kerem *et al.*, 1989; MacDonald *et al.*, 1993). Therefore, gene therapy has the potential to treat diseases by manipulating genes to silence (faulty) gene expression, to restore gene function, or to insert an exogeneous therapeutic transgene (Cox *et al.*, 2015; Kay, 2011; Vaishnaw *et al.*, 2010; Foldvari *et al*, 2016). The complexity of cells and tissues poses a barrier to efficiency of gene transfer. In therapies for CNS disorders, the BBB is also a limitng factor. Therefore, the success in any therapy will rely on the efficiency of the delivery system in crossing the BBB and delivering a DNA cargo after systemic administration (Jayant *et al.*, 2016; Upadyay, 2014; Misra *et al.*, 2003; Timbie *et al.*, 2015; Bourdenx *et al.*, 2014; Jayant and Nair, 2016).

Gene therapies have been developed over the past two decades focused in monogenic and recessive disorders. Specifically, been the basis for successful therapies involving the hematopoietic system (Naldini *et al*. 2015; Cox *et al.*, 2015; Gaspar *et al.*, 2011; Howe *et al.*, 2008; Aiuti *et al.*, 2013). These diseases have a known molecular background, such as hereditary diseases, cancer, and chronic infections (Naldini *et al*. 2015). Phase I/II clinical trials on thalassemia, hemophilia and retinal dystrophy are some of the diseases where gene therapy has proven efficacious and safe (Naldini *et al*. 2015). An optimized vector must have the following characteristics: (i) protection of the DNA cargo from degradation until its internalization in the nuclei of cells (ii) effectiveness; (iii) specificity for a given substrate; (iv) long-term expression; (v) low immune response; (vi) safety; (vii) accessibility; (viii) low cost (Jayant *et al.*, 2016).

Depending of the origin of the vector, gene therapy is branched in two main sub-categories – non-viral and viral gene therapy.

1.2.1 Non-viral gene therapy

Non-viral gene therapy consists of molecules that can transfer a gene into a cell (Jayant *et al.*, 2016). The most common methods are cationic polymers, cationic lipids, engineered polymers, nanoparticles, and naked DNA (Jayant *et al.*, 2016; Ramamoorth and Narvekar, 2015). These molecules form complexes or nanoparticles that involve the nucleic acids (Foldvari *et al*, 2016).

Non-viral methods are more efficient in localized, non-invasive therapies, for instance dermatological, pulmonary or mucosal targets, since they are more accessible and easy to target (Foldvari *et al.*, 2016). These methods are safer and cost-effective, compared to viral vector-based gene therapy (Foldvari *et al.*, 2016). The main disadvantages of these therapies are the short-term expression, and the fact that these therapies showed less efficiency in gene delivering compared to viral gene methods (Foldvari *et al*, 2016; Jayant *et al.*, 2016).

1.2.2 Virus-based gene therapy

In early stages of gene therapy, mammalian virus-based vectors proved to be an efficient vehicle to carry genes of interest (Kotterman *et al.*, 2015). The pathogenicity of a virus can be removed, by the elimination of viral genes, retaining the capacity and efficiency of gene transfer carrying a therapeutic gene, originating a viral vector (Naso *et al*, 2017; Robbins and Ghivizzani, 1998). In 1999, during a clinical trial using adenovirus (Ad) to treat ornithine transcarbamilase defiency, a patient died due to systemic inflammation and organ failure, leaving gene therapy in a hiatus (Kotterman *et al.*, 2015). However, with modern technologies and recent research, viral gene therapy returned to the spotlight.

Nowadays, viral gene therapy is widely used, due to the success as viral vectors of lentivirus and adeno-associated virus (AAV) (Kotterman *et al.*, 2015; Jayant *et al.*, 2016). The latter is considered to be the safest option since it is a non-pathogenic virus (Jayant *et al.*, 2016; Samulski and Muzyczka, 2014). These vectors have a high efficiency of transduction and are proved to have long-term expression, being more efficient than non-viral vectors (Jayant *et al.*, 2016; Bouard *et al.*, 2009).

The life cycle of a wild-type virus starts with infection of the host cell, followed by the replication of the viral genome, capsid production, packaging of the viral genome, and ending with the lysis of the cell and releasing of the viral particles (Samulski and Muzyczka, 2014; Bourdenx *et al*., 2014; Naso *et al*., 2017). The viral vectors take advantage of the wild-type lifecycle and are engineered by removing the viral genes and retaining the packaging signals (Kotterman *et al.*, 2015). The viral genes that encode for replication and structure are provided in *trans*, generating mechanisms to deliver the gene of interest without the pathogenicity, the viruses can then be used as vectors for therapeutic ends (Choudhury *et al*., 2017).

Currently, there are several viral vector types developed and with therapeutic interests (Table 1). In the following sections the major vectors types are briefly discussed.

Table 1. Viral vectors for gene therapy (adapted from Choudhury *et al*.,2017)

	Adenovirus	**Lentivirus**	**AAV**	**Retrovirus**	**Herpes Simplex Virus**
Packaging capacity	36 kb	7-9 kb	4.5 kb	7-8 kb	50-150kb
Genome	dsDNA	ssRNA	ssDNA	ssRNA	dsDNA
Coat	Naked	Enveloped	Naked	Enveloped	Enveloped
Transgene expression	Transient expression	Long term expression	Long term expression	Long term expression	Long term expression
Genome integration	Non integrative	Integrative	Non integrative	Integrative	Integrative and non-integrative
Tropism	Dividing and non-dividing cells	Dividing and non-dividing cells	Dividing and non-dividing cells	Dividing cells	Dividing and non-dividing cells

1.2.2.1 Adenovirus

These viruses belong to the *Adenoviridae* family and present a non-enveloped double stranded DNA genome. Ad enters the cells by endocytosis, but the virus developed a strategy to avoid the lysosome/endosome compartment. Ad vectors have a large packaging capacity, and are capable of carrying a 36 kb transgene. These vectors do not integrate in the genome and when injected in the parenchyma of a tissue are able to scatter and transduce broad number of cells. The drawback of Ad vectors is that the innate immune response is severe, leading to inflammation and cytotoxicity, since the organism can present pre-existing immunity. Ad vectors are normally used in cancer trials. Concerning CNS disorders, it has been used principally research on for brain tumor therapies. Ad vectors are also used for vaccination, by taking advantage of the immune response generated (Choudhury *et al*., 2017; Jooss and Chirmule, 2003; Crystal, 2014).

1.2.2.2 Lentivirus

Lentivirus are members of the *Retroviridae* family, derived from human immunodeficiency viruses (HIV). Lentiviral vectors (LV) are able to transfect both dividing and non-dividing cells, entering the cell by fusion of the envelope with the plasma membrane,delivering its contents into the cytoplasm, followeb by a release of the genome from the capsid, and integrating the transgene in the host cell genome (Choudhury *et al*., 2017). The packaging capacity of the vector is up to 8,5 kb. LV are capable of long-term expression, and since it integrates the genome, the therapeutic transgene is inherited by the progeny. The drawbacks of LV are its large size that prevents a wide biodistribution of the vector, and the immune innate responses by the host organism, although improvements in these vectors were made to increase the safety of the vector (Choudhury *et al*., 2017; Escors and Breckport., 2015), for example the development of non-integrating lentiviral (NIL) vectors, that persists in an episome, decreasing the risk of mutation caused by integration of the viral genome. LV are the second most common vector for gene delivery in the CNS, mainly in AD and Parkinson's disease (Lentz *et al.,* 2012).

1.2.2.3 Retrovirus and Herpes Simplex Virus

Retrovirus and Herpes Simplex Virus (HSV) are also vectors used in gene therapy, although their usage is less frequent. Retrovirus are derived from Moloney murine leukemia virus. This virus is not able to transfect non-dividing cells, compromising its use to treat CNS-related disorders. Instead, they are normally used for lineage determination in embryos (Choudhury *et al*., 2017). Retrovirus-based vectors show similarities with LV regarding packaging capacity and transfection mechanism, but the production of this virus has lower titers. HSV vectors are able to transfect neurons among other cell types and are able to either integrate into the genome of the host cell, or to as persist as episomes. The interesting characteristics of these vectors are that they can deliver a transgene up 150 kb in size and are produced with a high titer. Moreover, this vector is able to transduce neurons among other cell types. Currently, there is no clinical study using these vectors, due to problems with toxicity and production. (Choudhury *et al*., 2017; Lentz *et al.,* 2012).

1.2.3 Adeno-Associated Virus

AAV are non-pathogenic and non-replicative viruses, belonging to the *Parvoviridae* family (Rincon *et al.*, 2018; Kotterman *et al.*, 2015). In fact, AAVs are dependent on other viruses to replicate. Wild-type AAV carries a 4,7 kb single stranded DNA genome. It is a non-enveloped virus, similar to Ad, and possesses an icosahedral capsid. The genome of wild-type AAV is

constituted of 3 open-reading frames (ORF), flanked by 2 inverted terminal repeats (ITR). ITRs function as an origin site of replication and as a signal for encapsidation. The *rep* ORF, responsible for viral replication signals, encodes 4 non-structural proteins, and has further functions regulating viral transcription, genome integration, and virion assembly. The *cap* ORF encodes 3 structural proteins that constitute the virus 60-mer capsid (VP1-3). The third ORF is within the *cap* ORF; it encodes the assembly-activating protein, whose function is to localize the individual capsid proteins and assemble then into the final capsid structure (Kotterman *et al.*, 2015).

Recombinant AAV vectors do not integrate the host genome (Naso *et al.*, 2017). In AAV vectors, the viral genes are removed and are replaced by an expression cassette containing the transgene flanked by the ITR (Kotterman *et al.*, 2015). To produce AAV vectors, the viral genes are provided in *trans* as well as the helper viral genes provided by adeno or herpesvirus (Kotterman *et al.*, 2015; Flotte, 2004; Naso *et al.*, 2017). AAV vectors give stable transgene expression, even in the absence of helper viral genes. AAV vectors are capable of transfecting dividing cells as well as non-dividing cells, such as neurons, persisting in the host cell as concatemers in stable episomes (in the absence of Rep), which makes them an interesting tool for CNS-related disorders (Choudhury *et al*., 2017; Kotterman *et al.*, 2015). Although AAV vectors are less immunogenic than other vectors, such as LV, they might cause a mild innate immune response, due to the capsid or the transgene, blocking the therapeutic activity of the vector (Kotterman *et al.*, 2015).

Currently, there are 11 naturally occurring AAV serotypes and over 100 different variants of these serotypes described (Kotterman *et al.*, 2015). An AAV serotype is determined by the amino acid sequence of VP1-3. The tropism, or the ability to transduce more efficiently a given tissue or cell type, depends highly on the capsid (Dodiya *et al.*, 2015; Jonquieres *et al.*, 2019). The ITR derived from the AAV2 serotype is the most commonly used as a genome template, since it was the first serotype identified (Naso *et al.*, 2017). Meanwhile, AAV serotype 9 (AAV9), unlike any other naturally occurring serotype, is able to cross the BBB and transfect the heterogeneous cells present in the brain after intravenous injection. Therefore it is one of the preferred serotypes used for CNS-directed gene therapy (Lykken *et al*, 2018).

In an attempt to optimize AAV9, Deverman and colleagues developed a strategy to effectively screen new capsids generated by inserting in AAV9 7 amino acids of randomized sequence between the amino acids 588 and 589, which are encoded in the *cap* gene. The capsids were produced by using the CRE-recombination based AAV target evolution method (CREATE) (Deverman *et al.*, 2016). The most enriched capsid, the PHP.B, encodes the amino acid sequence TLAVPFK (Deverman *et al.*, 2016). It was proved PHP.B provided a higher efficiency in gene transfer due to an improved capacity to efficiently cross the BBB, increasing the bioavailability of the vector in the CNS improving the final transduction levels without significant off-target effects, after systemic injection (Rincon *et al.*, 2018; Deverman *et al.*, 2016).

AAV genome replication depends entirely on the resolution of the hairpins formed in the ITRs. A complex of replication, containing the host polymerase binds to one of the ITRs. On the other ITR, an endonuclease Rep nicks the ITR at the terminal resolution site, followed by the elongation of the molecule by the replication complex, replicating a single-stranded (ss). The ssAAV conformations needs to be converted in a double-stranded conformation in order to start the transcription, which is a limiting step of the gene expression, since some cell types have a limited ability to synthesize a double stranded DNA from a single stranded genome (McCarty *et al.*, 2008;

Rincon *et al.*, 2018).The self-complementary (sc) conformation can overcome this limiting step, providing an increased efficiency and increased speed of transgene expression. The sc conformation is formed when Rep fails to nick the terminal resolution site, due to the deletion of this sequence in one of the ITR. The replication complex reaches the mutated terminal resolution site and continues to elongate through the ITR and copies towards the initial ITR. After the initial replication cycle, the end product is a DNA molecule with 2 wild-type ITRs at the ends, and a mutated ITR in the middle of the molecule. The single stranded DNA molecule has two regions that self-complement, therefore the molecule can fold and form a double stranded molecule (McCarty *et al.*, 2008). Typically, the wild-type AAV genome is packaged in an ssDNA conformation. After uncoating, the genome anneals and forms a double-stranded DNA molecule. Therefore, in order for the scAAV conformation to be packaged with a single stranded genome, the effective size has to be reduced to 2500 bp, or 2200 bp for the transgene and about 145 bp for the ITR.

An ideal vector must provide long-term correction of the disorder with one single, non-invasive treatment (Lykken *et al*, 2018). Additionally, with systemic delivery systems for CNS-directed targets there are increased difficulties compared to other targeted therapies, such as the liver and heart (Deverman *et al.*, 2016). In CNS-targeted therapies, to reach a therapeutic effect, a large and heterogeneous area of the brain must be targeted (Rincon *et al.*, 2018). Therefore, developing effective tools is a clinical priority; for example, the use of optimized capsids that efficiently transduce brain cells, such as PHP.B, along with the development of novel therapeutic transgenes, such as antibodies that provide a high specificity and high potency. This strategy, also known as vectored immunoprophylaxis (VIP), has shown itself to be very stable and substrate-specific, and is discussed in detail in the next section.

1.3 Vectored Immunoprophylaxis

VIP consists in the passive immunization by viral vector-mediated delivery of transgenes encoding neutralizing antibodies into non-hematopoietic cells (Sanders and Pozio, 2017; Deal *et al.*, 2015). This approach has been successfully used to treat mouse models of HIV, malaria, and influenza (Sanders and Pozio, 2017; Deal *et al.*, 2014; Balazs *et al.*, 2011; Balazs *et al.*, 2013). There has been an increasing interest in passive immunization for instances, to treat Ebola virus using monoclonal antibodies (Sanders and Pozio, 2017). In a direct injection of monoclonal antibodies (mAb), to achieve a therapeutic effect, the mAb must be provided in high concentrations due its short lifetime, requiring multiple injections. Viral vectors allow the efficient and rapid delivery of the transgene, moreover, the vector can be engineered in order to achieve a higher tropism to a cell type or tissue (Sanders and Pozio, 2017). Hence, the delivery of antibodies mediated by a viral vector may lead to endogenous production and a sustained expression of the protein after just one injection (Sanders and Pozio, 2017).

Concerning VIP therapies for CNS conditions, when produced in the peripheral muscle and secreted, the mAb activity in the brain was inefficient. This was probably due to the large size of the mAb (typically in the region of 150 kDa), the poor biodistribution of penetrating mAb throughout the brain parenchyma, high microglia-mediated immunogenicity (Zafir-Lavie. *et al.*, 2018; Bannas *et al*., 2017; Freskgard and Urich*,* 2017; Wang *et al.,* 2016; Panza *et al.,* 2014). Therefore, local production of antibodies is the most attractive option to achieve a therapeutic response. However, the reduced size of transgene that can be carried by a scAAV vector is typically much smaller than the coding sequence of a standard antibody, consequently smaller proteins are better suited for a scAAV-based strategy, like single-chain variable fragments (scFV)

or nanobodies. Typically, scFV antibodies tend to show lower affinities for their target than their parent templates (Niewoehner *et al*., 2014), considerably limiting their use as therapeutics. This challenge can be overcome by employing nanobodies, a technology pioneered at the Vlaams Instituut voor Biotechnologie (VIB) and the Vrije Universiteit Brussels (VUB).

Nanobodies are constituted by a small single variable antigen binding domain, with a size of around 120 amino-acids and a molecular weight of about 15 kDa (Zhou *et al.*, 2011). These molecules are produced by immunizing a camelid, followed by isolation of the immune cells to produce a library of nanobodies, that are further selected based on desired characteristics, such as high affinity and potency (Wagner *et al*., 2018). Nanobodies have some interesting features, such as stability, high specificity, high affinity to small antigens that are unavailable to mAbs, and the lack of the Fc region reduces the immunogenicity compared to standard mAbs (Hassanzadeh-Ghassabeh *et al.*, 2013). Moreover, nanobodies can easily be engineered by fusion to other proteins or to signal sequences. The drawbacks of these small molecules are rapid renal clearance due to its size and limited BBB permeability after systemic delivery (Steeland *et al.*, 2016; Bannas *et al.*, 2017). Unfortunately, when administered systemically *in vivo,* an anti-BACE1 nanobody showed no significant decrease in Aβ content (Terryn *et al.*, 2014). Hence, the need to produce a nanobody that provides anti-BACE1 activity by decreasing the Aβ content and a more efficient delivery system arised. The delivery of a nanobody by an AAV vector in order to transduce brain cells efficiently and achieve high local concentrations of nanobody is promising. The small size of the nanobody allows it to be cloned into a scAAV plasmid, a conformation that boosts transgene expression of the transgene (Rincon *et al.*, 2018) and allows long-term expression of the nanobody (Zafir-Lavie *et al.*, 2018).

Our work is focused on the establishment of a novel AAV-based therapy by using a specific anti-BACE1 nanobody, named B9, which was tested *in vitro*, showing decreasing levels of Aβ in mammalian cells bearing the APP^{NL} mutation (US8568717B2, https://patents.google.com/patent/US8568717B2/en). To achieve this purpose, we designed an ssAAV vector containing a hybrid cytomegalovirus/chicken β-actin (CBA) promoter driving the expression of the B9 nanobody. Additionally, the woodchuck post-trasnscriptional regulatory element (WPRE) was cloned into the transgene cassette together with SV0 poly-A (pA), which stabilizes the messenger RNA (mRNA). The nanobody is fused to an N-terminal BACE1 signal-peptide, which potentially increases the nanobody binding to BACE1 by maximazing their interactions, since they would be distributed in the same pathway, and to a C-terminal c-myc tag, that allows *in vivo* detection of nanobody expression. Moreover, we attempted to boost the B9 expression by administering a scAAV vector carrying the nanobody. Therefore we designed a scAAV conformation that potencially enables a faster production of the transgene compared to the ssAAV (Rincon *et al.*, 2018). The main drawback of the scAAV conformation is the packaging capacity, which is half the capacity of the ssAAV conformation (McCarty *et al.*, 2008). Therefore, to obtain a transgene inside the capacity range, we had to remove the WPRE from the transgene cassette. The role of the WPRE was reported to stabilize the mRNA (Sun *et al.*, 2009; Wang *et al.*, 2016).

2 Project Aims

Ultimately, the goals of this work are:

- The evaluation of the anti-BACE1 nanobody B9 activity using multiple murine strains after systemic delivery of a ssAAV-PHP-B-CBA-B9 –WPRE viral vector.
- To compare the expresssion levels of B9 of an AAV vector with a single stranded transgene cassette - ssAAV-PHP.B-CBA-B9-WPRE, and an AAV vector with self-complementary transgene cassette - scAAV-PHP.B-CBA-B9 without the WPRE sequence.

3 Materials and Methods

3.1 Plasmid production and purification

SURE2 supercompetent *E. coli* cells (Agilent technologies, 200152), were used for transformation of the plasmids pHelper, pPHP.B and pAAV-CAG-B9. The plasmids are ampicillin resistant. Transformations were performed accordingly to the following protocol: 50 µl of SURE 2 cells were mixed with 2 µl of plasmid. The tube containing the cells was kept on ice for 30 minutes, followed by an incubation step of 30 seconds at 42ºC, before placing once again on ice for 2 minutes. Afterwards, the cells were grown in super optimal broth with catabolite (SOC) medium (New England Biotech, B9020S) at 37ºC and continuous shaking at 250 rpm for 1 hour. 50 µl of cells were then plated on a lysogeny broth (LB) medium agar plate containing 100 µg/ml ampicillin and left to grow overnight at 37ºC. The following morning, a single colony was picked and cultured in 5 ml of LB medium supplemented with 100 µg/ml ampicillin for 7 hours at 37ºC, with continuous shaking at 250 rpm. After the incubation step, the culture was seeded at a 1/1000 dilution in 1 L of terrific broth (TB) or LB medium, accordingly to the expected copy number per host cell of each plasmid. The medium was supplemented with ampicillin at a concentration of 100 µg/ml. The cultures was incubated overnight at 37ºC and 250 rpm. Afterwards, cells are pelleted by centrifugation at 5000 g for 15 minutes (Beckman Coulter, Avanti J-C). Plasmid DNA was extracted with the QIAGEN Megaprep kit (12181) following the manufacturer's instructions. Concentration and purity of the plasmid DNA samples was assessed by measuring the absorbance at 260 nm and by measuring the 260/280 nm ratio, respectively (Nanodrop Technologies, Rockland, Delaware, USA). Plasmid DNA samples were stored at -20ºC.

3.2 Cloning of plasmids

In the cloning of pscAAV-CAG-B9, the plasmid was cloned by a two-step cloning strategy. The backbone plasmid was selected to later produce a vector with the self-complementary genome configuration. pscAAV-CBA-eGFP was digested with the restriction enzymes KpnI and Hind III (New England Biotechnology, R0142S and R0104S), to remove the CBA-eGFP sequence. Meanwhile the CAG promoter was isolated by digestion with the same enzymes from a pssAAV-CAG-B9 (from Todd Golde's lab). For the restriction digest, 500 ng of plasmid DNA were incubated with 0,5 ul of each restriction enzyme and 2 µl of the appropriate enzyme buffer for 3 hours at 37ºC. The DNA fragments obtained were run in a 1% agarose gel for 40 min at 120 V to ensure separation of the fragments of interest. pscAAV and the CAG promoter were then isolated from the gel and purified with the QIAquick gel extraction kit (QIAGEN, 28704) following manufacturer's instructions.

The pscAAV backbone was dephosphorylated by Calf Intestinal Phosphatase (CIP, New England Biotech M0290), according to the manufacturer's instructions. The backbone and the fragment of interest were then ligated using PCR. SURE2 cells were transformed as described above, and the colonies screened by PCR, with the following conditions: initial step of 2 minutes at 95ºC, and then 35 cycles of 15 seconds at 95ºC, 30 seconds at 54ºC and 50 seconds at 72ºC, finalized by a step of 5 minutes at 72ºC. The plasmid DNA of the colonies that transformed with pscAAV-CAG was purified with a QIAGEN Miniprep kit (27104), following the manufacturer's instructions. Plasmids were verified by sequencing.

In a second step, the B9 nanobody with the BACE1 signal peptide and cmyc-tag was amplified from pssAAV-CAG-B9 using PCR. The protocol used was an initial step of 1 minute at 95ºC, and then 35 cycles of 15 seconds at 98ºC, 30 seconds at 60ºC and 40 seconds at 72ºC, finalized by a step of 5 minutes at 72ºC, using the primers (forward 3'-TATTGTGCTGTCTCATCATTTTGGCAAAGAATTGGATCAAAGCTTGGTACCGAGCT-5' and reverse 3'-GTCGAGGCTGATCAGCGAGCTCTAGTCGACGGTATCGATATCGATAAGCTGCTCGAGGCG-5'). The backbone plasmid pscAAV-CAG was linearized using a 3 hours incubation with the restriction enzyme HindIII at 37ºC. The linearized backbone and the B9 fragment were later assembled using the NEBuilder Assembly HIFI kit (New England Biotechnology, E2621), with an incubation step of 15 min at 50ºC. The successful assembly of the construct was verified as described above.

3.3 AAV production and purification

Production of AAV vectors employed in the experiment described in this thesis was outsourced to ViGene Bioscience (Rockville, MD,USA).

3.4 Animal procedures

In the project, the following mouse strains were used: C57Bl/6 (Jackson Laboratory, Bar Harbor, ME), APP^{Dutch}, APP^{NL-G-F} and APP/PS1.

The APP^{Dutch} strain is a transgenic model that bears the Dutch mutation (APP693Q), which alters the processing of APP (Herzig *et al.*, 2004). APP^{Dutch} mice develop a form of cerebral amyloid angiopathy (CAA), with a phenotype characterized by severe hemorrhages and amyloid deposition in the cerebral vessels (Timmers *et al.*, 1990). There are no plaques formation in this strain and CAA develops at 22-24 months of age (Herzig *et al.*, 2004). The APP^{NL-G-F} is a knock-in model that bears 3 mutations: APP KM670/671 NL (Swedish), APP I716 F (Iberian) and APP E693G (Artic) (Sakakibara *et al.*, 2018). Each mutation has an effect on the properties of Aβ production, deposition and toxicity: the swedish mutation increases the Aβ production, the iberian one increases the ratio Aβ42/Aβ40, and the artic mutation promotes the Aβ aggregation (Sakakibara *et al.*, 2018). This model is characterized by aggressive amyloidosis, and Aβ deposition at early stages (Saito *et al*., 2014). APP/PS1is a transgenic model bearing the APP KM670/671 NL mutation, and the PSEN1 L166P mutation. The expression of transgene APP is 3-fold higher than the endogenous APP, and a high ratio of Aβ42/40. This model is characterized by an aggressive amyloidosis, and plaque formation in the cortex at 6 weeks of age and 3-4 months in the hippocampus (Radde *et al.,* 2006).

The mice have been employed to test the efficacy of the therapeutic nanobody by reducing the amyloid load. The vector was administered *via* tail vein with a dose of $1x10^{12}$ vector genome (vg)/mice (total volume of 100 µl) of each AAV vector. The injection of APP^{Dutch} mice was performed at 13 weeks of age. The analysis of brain samples was performed 4 weeks after injection. The APP^{NL-G-F} mice received the vector at 6 or 16 weeks of age. The analysis of brain samples was performed at 18 or 21 weeks of age, accordingly. The APP/PS1 mice were administered at the age of 6 weeks. The analysis of brain samples was performed 16 weeks of age.

For the experiment of comparison between the ssAAV-CBA-B9-WPRE vector and the novel scAAV-CBA-B9 vector, APP^{Ducth} mice were used. The vector was administered *via* tail vein with a dose of $1x10^{12}$ vg/mice (total volume of 100 µl) of each AAV vector. The injection of the APP^{Dutch} was performed at 6 weeks old. The analysis of brain samples was performed 4 weeks after injection. The C57Bl76, untreated, have been employed only to provide a baseline of protein expression for the Mass Spectrometer analysis. Therefore, they were sacrificed at the age of 10 weeks to age-match the groups treated with the vector. Before harvesting the brain samples, all the animals were injected intra-peritoneally (IP) with Dolethal (Vetoquinol, UK) to induce sedation. The mice were then transcardially perfused with ice-cold phosphate buffered saline (PBS). The brain was collected, and the right hemisphere was post-fixated in 4% paraformaldehyde (PFA) overnight. 50 µm brain sections were obtained by a vibrating microtome (LEICA VT1000S). The left hemisphere was dissected to isolate the cortex, the hippocampus, and the midbrain regions. The samples were snap-frozen separately in liquid nitrogen and stored at -80ºC until further processing.

3.5 Extraction of soluble and insoluble protein

In order to later quantify the content of Aβ peptides in the different brain regions, extraction of the soluble and insoluble fractions of Aβ is performed.

For the soluble fraction, around 35 mg of cortex tissue or the whole hippocampus are homogenized, in FastPrep tubes (Lysing Matrix D, MP Biomedical, (MP116913050) after addition of an extraction buffer. The buffer composition is 10 ml of Tissue protein extraction reagent (T-PER, PIERCE, 78510), 1 tablet complete mini protease inhibitor (PI, Roche, 11836153001), 100 µl of Phosphatase inhibitor cocktail 2 (Sigma-Aldridge, P5726-1ML) and 100 µl of Phosphatase inhibitor cocktail 3 (Sigma-Aldridge, P0044-1ML). The buffer is added to the tube, 10x the equivalent volume based on tissue weight. The samples are then homogenized for 45 sec 6.5 m/s, using a MP Fastprep-24 tissue and cell homogenizer. The homogenized samples were spun down for 5 min, 5000 g at 4ºC, and the supernatant transferred to Beckman ultracentrifugation tubes. Samples were centrifuged for 1 hour, at 4ºC and 131440 g (Beckman Ultra Optima TLX). The supernatant (soluble fraction) was collected and transferred to a new tube. Both the supernatant and the pellet, later used to obtain the insoluble fraction, are stored at -80ºC.

For the insoluble fraction, the aforementioned pellet is resuspended in 6M GuHCl (ThermoFisher, 24110) with PI, 2x equivalent volume based on the pellet weight, and then sonicated for 30 seconds, 10% amplitude, using a Branson Digital sonifier. After sonication, samples are vortexed and incubated for 1 hour at 25ºC. At the end of the incubation step, the supernatant is transferred into screw-cap tubes (Starstedt) and centrifuged for 20 minutes, at 4ºC and 212911 g. The supernatant is then collected and diluted 12x in GuHCl diluent buffer (20 mM phosphate, 0,4 M NaCl, 2mM EDTA, 0,05%(w/v) NaN_3 and 0,075%(w/v) 3-[(3-Cholamidopropyl) dimethylammonio]-1-propanesulfonate (CHAPS)

3.6 Protein determination

To ensure that the same total amount of protein per each sample is loaded on the ELISA plate, protein content is measured based on the methods previously described (Lowry *et al*., 1951; Peterson *et al.,* 1977). In summary, the total amount of protein in the sample is determined by using a standard curve of known concentrations of bovine serum albumin (BSA, ThermoFisher).

To allow protein precipitation, 100 µl of 0,15%(w/v) deoxycholate (DOC) (Thermo Scientific) and 100 µl of 72% trichloroacetic acid (TCA) (Thermo Scientific are added to the samples and the BSA standards (1ml final volume). Samples are carefully vortexed and incubated for 10 minutes on ice. After the incubation, samples are centrifugated for 10 minutes, 4ºC and 16200 g in a Heraeus Fresco 21 Microcentrifuge. Afterwards, the supernatant is gently aspired and the pellet resuspended in 250 µl ddH_2O and 750 µl of a solution containing Na_2CO_3, NaOH, Na_2-Tartratex_2H_20, SDS, $CuSO_4x5H_20$, and incubated at room temperature for 30 minutes. Then, 75 µl of Folin-Ciocalteus-Phenol-Reagent (Merck 9001) was added, immediately mixed and incubated for 45 minutes at room temperature. The absorbance was measured at 750 nm in a spectrophometer (Thermo-Scientific).

3.7 Quantification Aβ peptides

The Aβ peptides were measured by performing a sandwich ELISA assay with the following protocol. Nunc maxisorp flat-bottom 96 wells plates (ThermoScientific, 44-2404-21) were coated with coating buffer (10 mM Tris-HCl, 10 mM NaCl, 10 mM NAN_3) supplemented with the capture antibody against human Aβ40 (JRF/cAbeta40/28) or Aβ42 (JRF/cAbeta42/26) provided by Janssen, at a final concentration of 1,5 µg/ml. The plates are incubated overnight at 4ºC on a tilting table.

The next morning, the coating buffer is discarded by quickly inverting the plate, and the wells were rinsed 5 times with 150 µl of PBS (Gibco) supplemented with 0,05% Tween20 (Sigma-Aldridge). The plates were blocked with PBS with 0,1% casein (PBS-casein, Sigma-Aldridge), and incubated at room temperature for 4 hours. To ensure that the same amount of total protein is loaded on the coated plate for all of the samples, they were diluted in PBS-casein to a standard concentration of 3 µg/µl for cortex, and 1,5 µg/µl for hippocampus. The samples were further diluted, depending on the strain, in order to ensure that the absorbance was inside the linear range of the standard curve.

After preparation of the appropriate dilutions, 30 µl of conjugated antibody huAB25-HRPO (Janssen), diluted at the concentration of 1/6000 in PBS-casein, were pipetted per well into a 96 wells PCR plate, non-skirted (VWR, 732-2879). Then, 30 µl of each sample dilution were added per well and mixed carefully with the conjugated antibody by pipetting up and down. When all the samples were loaded, dilutions at a known concentration of the appropriate Aβ peptide were prepared as a standard curve and loaded in the PCR plate. The content of the plate was mixed on a plate shaker for 5 minutes at 1000 rpm. To ensure that the full content of the plate was at the bottom of each well, a centrifugation step of 5 minutes, 1000 rpm was performed. 30 µl of each well were then loaded in the coated Nunc maxisorp plate, and incubated overnight at 4ºC on a tilting table.

The following morning, the sample-antibody mix were discarded, and the wells were rinsed 5 times with PBS supplemented with 0,05% Tween20. During the last wash, the developing solution containing 6 ml of 100mM NaAc (Sigma Aldrich) pH4.9, 60 µl of 3,3′,5,5′-Tetramethylbenzidine (TMB, Sigma Aldrich) and 6 µl of 30% H2O2 (Sigma Aldrich) was prepared. 50 µl of developing solution was pipetted in each well. The plate was then incubated for 8-10 minutes in the dark.

After the incubation, 2N H_2SO_4 was added to stop the colorimetric reaction, and the absorbance measured at 450 nm in a Perkin Elmer EnVision 2103 Multilabel reader.

3.8 Immunohistochemistry

50 μm thick sagittal brain sections were washed for 10 minutes with Tris buffered saline (TBS) (50 mM Tris-Cl, 150 mM NaCl mM, pH 7.6) in a 24 well plate (VWR). 500 μl of the blocking solution containing 1% Triton X-100 in TBS with 10% normal donkey serum (NBS) (Abcam) were added to each well and the plate is stored at room temperature for 1 hour on a tilting table. The primary antibodies (Rabbit anti-cMyc tag to produced by Sigma-Aldrich #C3956, to identify the nanobody, diluted 1:500; Guinea pig anti-Neun, Sigma-Aldrich #ABN90, diluted 1:400) were diluted in the blocking solution. 500 μl of the primary solution are added to each well. The plate were stored overnight at 4ºC on a tilting table. The following morning, the brain sections were washed with TBS 3 times and incubated with 500 μl/well of the secondary antibody solution (Donkey anti-guinea pig Cy5, Jackson Immuno #706-175-148; Donkey anti-rabbit Alexa488, Invitrogen #A21206, added to the blocking solution at a dilution of 1:200 and 1:500 respectively). The plate was incubated for 1 hour at room temperature on a tilting table. Sections are then rinsed with TBS and mounted with Fluromount-G containing with DAPI (Thermo Scientific, 4959-52). The sections were imaged with a Leica DM5500 epifluorescence microscope with the objectives APO5x/0.07 and APO2.5x/0.15.

3.9 Shotgun LC-MS/MS

The following brain regions were sent to the VIB Proteomics Core to be analysed: Right cortex of C57Bl6 noninjected, and C57Bl6/APP^{Dutch} injected with ssAAV-PHP.B-CAG-B9-WPRE and scAAV-PHP.B-CAG-B9. Tissue samples were processed with the iST kit (PreOmics, Germany, P.O.00001). The B9 expression was measured by liquid chromatography coupled to mass-spectometry in tandem (LC-MS/MS). LC-MS/MS runs on all 9 samples were searched together using the MaxQuant algorithm (version 1.6.3.4) with default search settings including a false discovery rate set at 1% on both the peptide and protein level.

3.10 Statistical analysis

Differences in Aβ concentration between the brain regions were determined using an unpaired *t-test* with Welch's correction. All statistical analysis was performed using GraphPad (San Diego, CA,USA).

4 Results

4.1 Evaluation of the nanobody activity in APP^{Dutch} mice

Anti-BACE1 nanobody (B9) activity was assessed by measuring the concentration of Aβ content post-injection on APP^{Dutch} mice. Two groups of mice were injected either with the ssAAV-PHP.B-CBA-eGFP-WPRE (control vector) or ssAAV-PHP.B-B9. This model is characterized by a high ratio of Aβ40/Aβ42 (Herzig *et al.*, 2004). Hence, only the Aβ40 fractions were measured in this assay. The animals were injected with a dose of $1x10^{12}$ vg/mice of vector through tail vein injection at 13 weeks of age and euthanized 4 weeks post-injection. The Aβ levels were measured by sandwich ELISA on the regions of interest, the cortex and the hippocampus, on both soluble and insoluble fraction.

An evident decrease in Aβ40 species post-delivery of the vector was detected in the soluble fractions, especially from the hippocampus region (Fig. 2a-b). In the insoluble fraction, a statistically significant decrease in the Aβ40 species was measured in samples obtained from the hippocampus, but not from the cortex (Fig. 2c-d).

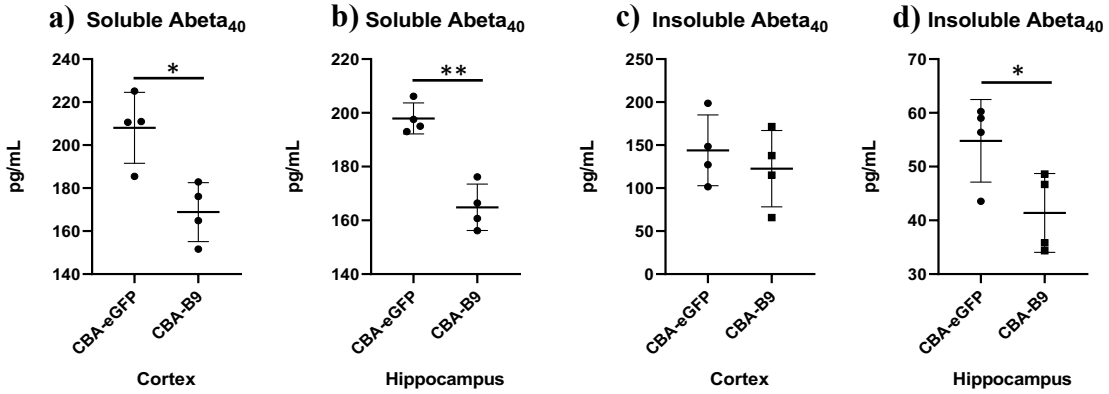

Figure 2. Decrease in Aβ species post-injection of ssAAV-PHP.B-CBA-B9 in APP^{Dutch}. Mice were injected with ssAAV-PHP.B-CBA-eGFP-WPRE and ssAAV-PHP.B-CBA-B9-WPRE at a dose of $1x10^{12}$ vg/mice. The Aβ content in the fractions of interest was measured. a) Soluble Aβ40 from cortex; b) Soluble Aβ40 from hippocampus, c) Insoluble Aβ40 from cortex, d) Insoluble Aβ40 from hippocampus. (n=4 per group) * $p<0.05$, ** $p<0.005$

Despite the promising results in APP^{Dutch}, this model does not develop cognitive changes or show plaque aggregation, which limits the potential readouts (behavioral and physiological) that can be used to assess the effect of B9 delivery. Therefore, we decided to assess the therapeutic efficacy of B9 in AD mouse models such as APP^{NL-G-F} and APP/PS1.

4.2 Evaluation of the nanobody activity in APP^{NL-G-F}

The assessment of the efficacy of B9 in different mouse models allowed to test the efficiency of this therapy across strains. Firstly, we assessed the efficiency of B9 in lowering Aβ levels in APP^{NL-G-F}. The Aβ levels were measured in two mouse groups injected with either ssAAV-PHP.B-CBA-eGFP-WPRE or ssAAV-PHP.B-B9, at a dose of $1x10^{12}$ vg/mouse. Injections were performed at 16 weeks old and mice were euthanized at 21 weeks of age. The Aβ content was measured by a sandwich ELISA, on the soluble fraction of Aβ40, obtained from cortex and hippocampus, and soluble Aβ42 fractions from the cortex region. The insoluble Aβ40 fractions from cortex and hippocampus regions, and soluble Aβ42 fraction from the hippocampus regions

are not represented due to low levels of Aβ in the fractions. A statistically significant decrease was detected in the soluble Aβ42 fraction obtained from cortex region following B9 administration. Moreover, analysis of the insoluble Aβ42 fractions showed no decrease, but there was a decreasing trend content on the soluble Aβ40 fractions (Fig. 3a-e).

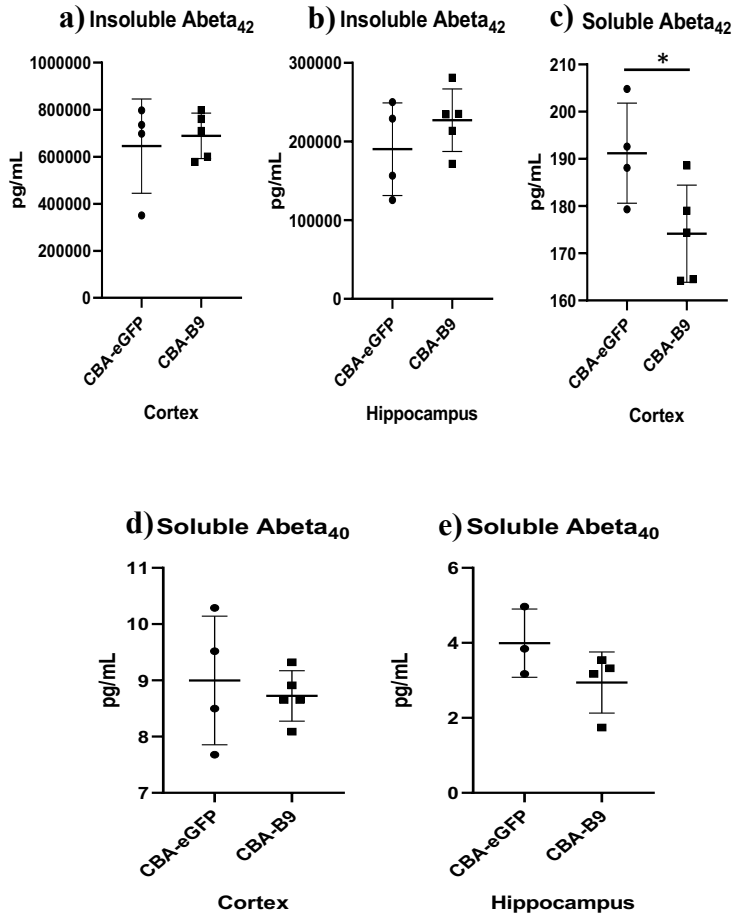

Figure 3. Aβ species did not decrease post-injection of ssAAV-PHP.B-CBA-B9 in APP^{NL-G-F}. Mice were injected with ssAAV-PHP.B-CBA-eGFP-WPRE and ssAAV-PHP.B-CBA-B9-WPRE with 1x10^{12} vg/mice. The Aβ content in the fractions of interest was measured. a) Insoluble Aβ42 fraction of the cortex; b) Insoluble Aβ42 fraction of the hippocampus, c) Soluble Aβ42 fraction of the cortex, d) Soluble Aβ40 fraction of the cortex, e) Soluble Aβ40 fraction of the hippocampus. (n=4 per group) * $p<0.05$

The levels of Aβ in the majority showed no statistically significant decrease in the analyzed samples, possibly due to the accumulation of Aβ deposits, that at age of analysis (16 weeks) in APP^{NL-G-F}, is already established. Therefore, the injection of mice at younger age, in which there are lower accumulation of Aβ deposits could unravel a therapeutic window.

4.3 Evaluation of the nanobody activity at younger age in APP^{NL-G-F}

To investigate whether age plays a role in the effect seen after B9 administration, Aβ levels were measured in two groups of mice injected at 6 weeks of age either with ssAAV-PHP.B-CBA-eGFP-WPRE or ssAAV-PHP.B-B9 (10x10^{12} vg/mouse). Mice were euthanized at 18 weeks of age. The Aβ content was measured by a sandwich ELISA, as before, insoluble fractions from cortex and hippocampus regions on both Aβ40 and Aβ42 species, and soluble Aβ42 fraction from

the cortex region. The remaining soluble fractions are not represented since the low Aβ levels on these fractions.

As expected, a statistically significant decrease in Aβ levels was detected in the insoluble Aβ40 fractions extracted from the hippocampus and cortex, as well as in the insoluble Aβ42 fraction obtained from the hippocampus region, which is the main constituent of the Aβ plaques (Fig. 4a-c). The insoluble and soluble Aβ42 fractions obtained from the cortex showed a minor decrease in Aβ levels, which could be due to the lower levels of Aβ present in the fraction (Fig. 4d-e). Nonetheless, a decreasing trend was observed in the majority of the fractions which led us to conclude that the B9 activity is sufficient to achieve a decrease in Aβ levels.

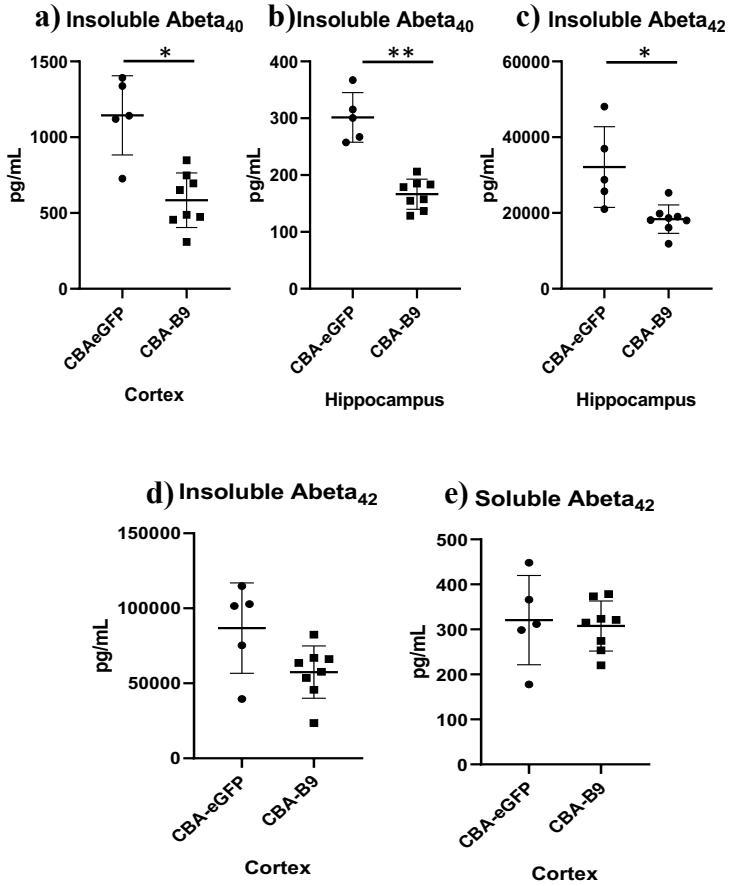

Figure 4. Aβ species showed a decrease post-injection of ssAAV-PHP.B-CBA-B9 in APP^{NL-G-F}. Mice were injected with ssAAV-PHP.B-CBA-eGFP-WPRE and ssAAV-PHP.B-CBA-B9-WPRE at a dose of $1x10^{12}$ vg/mouse. The Aβ content in the fractions of interest was measured. A) Insoluble Aβ40 from the cortex; b) Insoluble Aβ40 fraction from the hippocampus, c) Insoluble Aβ42 fraction from the hippocampus, d) Insoluble Aβ42 fraction from the cortex, e) Soluble Aβ42 fraction from the cortex. (n=4 per group) * $p<0.05$, ** $p<0.005$

4.4 Evaluation of the nanobody activity in APP/PS1

The APP^{NL-G-F} strain is still being characterized, and there are contradictory results regarding behavioral changes in the strain (Latif-Hernandez *et al*., 2019). Meanwhile, if Aβ is reduced after injecting the vector, it would be expected to decrease the disease severity, which would manifest itself in behavioral testing. Therefore, we tested the efficiency of B9 in a the APP/PS1 model,

which has a known behavioral phenotypes (e.g. Morris Water Maze and passive avoidance) (Radde *et al.*, 2006).

Due to the high severity of amyloidosis in this strain, mice were immediately injected at a young age (6 weeks), in order to measure Aβ levels before the plateau levels of deposit is achieved. Aβ levels were measured in two injected groups: one was injected with ssAAV-PHP.B-CBA-eGFP-WPRE and a second injected with ssAAV-PHP.B-B9. The dose used was $1x10^{12}$ vg/mouse. Mice were injected at 6 weeks of age, and euthanized 10 weeks later. The Aβ content was measured as previously described, insoluble fractions from cortex and hippocampus regions on both Aβ40 and Aβ42 species, as well as in the soluble Aβ42 from cortex and hippocampus regions. The represented fractions are the ones where the levels of Aβ were measurable. Unfortunately, there was no significant decrease observed in any fraction (Fig. 5a-f).

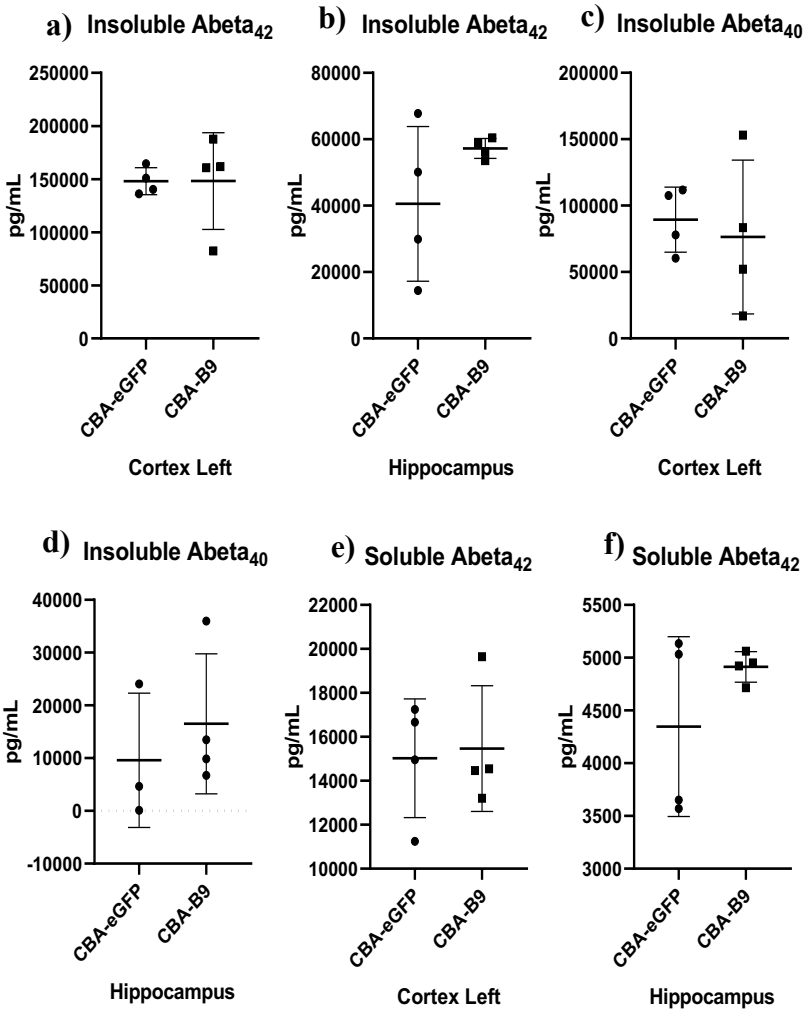

Figure 5. Aβ species in the APP/PS1 were not reduced by treatment with ssAAV-PHP.B-CBA-B9. Mice were injected with ssAAV-PHP.B-CBA-eGFP-WPRE or ssAAV-PHP.B-CBA-B9-WPRE at a dose of $1x10^{12}$ vg/mouse. The Aβ content in the fractions of interest was measured. a) Insoluble Aβ42 fraction from cortex; b) Insoluble Aβ42 fraction from hippocampus, c) Insoluble Aβ40 fraction from cortex, d) Insoluble Aβ40 fraction from hippocampus, e) Soluble Aβ42 fraction from cortex, f) Soluble Aβ42 fraction from hippocampus. (n=4 per group)

4.5 Comparison of scAAV-PHP.B-CBA-B9 and ssAAV-PHP.B-CBA-B9

The lack of B9 efficiency may be due to the insufficient production of the nanobody comparing the high levels of production of the Aβ peptides. Therefore, we attempted to boost the B9 expression by administering a scAAV vector carrying the nanobody.

For this experiment, APP^{Dutch} mice were used, since B9 was shown to reduce Aβ in this mice strain under specific conditions (see Fig. 2). Due to time constraints, however, mice were injected at a younger age int his set of experiment, although the time between injection and euthanasia was kept constant. The concentration of Aβ species was measured in 3 injected groups – a group injected with ssAAV-PHP.B-B9-WPRE, a group of scAAV-PHP.B-B9, and the control group injected with ssAAV-PHP.B-eGFP Each mouse received a dose of $10x10^{12}$ vg at 6 weeks of age and were sacrificed 4 weeks later.

The Aβ content was measured by a sandwich ELISA, as previously described, on soluble Aβ40 and soluble Aβ42 fractions of the cortex and hippocampus regions, since only these fractions levels of Aβ in the detection range. In this assay, no statistically decrease was observed between the groups (Fig. 6a-d), possibly due to the low concentration of Aβ species present in the regions of interest at the age of analysis. However, a clear trend in decreasing content in the group injected with the ssAAV-PHP.B-CBA-B9-WPRE compared to the control group on the fractions from the hippocampus region.

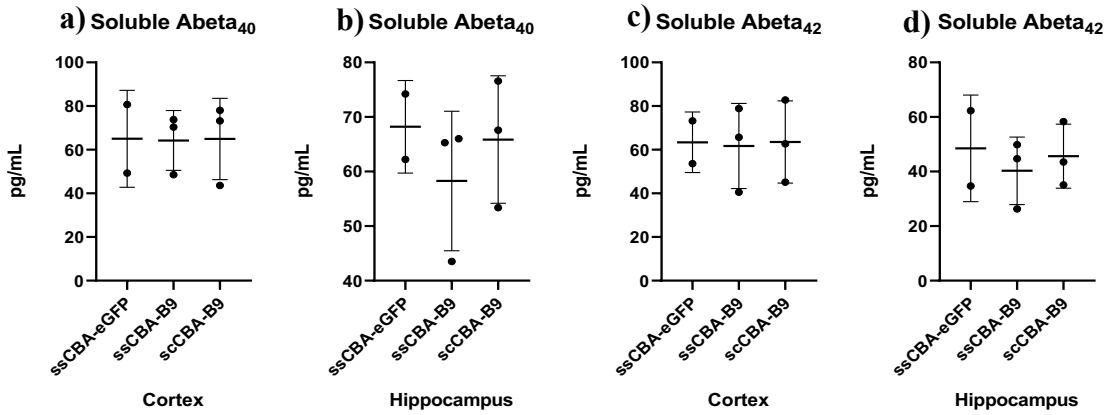

Figure 6. Aβ species did not decrease post-injection of ssAAV-PHP.B-CBA-B9-WPRE or scAAV-PHP.B-CBA-B9 in APP^{Dutch}. Mice were injected with ssAAV-PHP.B-CBA-eGFP-WPRE, ssAAV-PHP.B-CBA-B9-WPRE, scAAV-PHP.B-CBA-B9 with $1x10^{12}$ vg/mice. The Aβ content in the fractions of interest was measured. a) Soluble Aβ40 fraction of the cortex; b) Soluble Aβ40 fraction of the hippocampus, c) Soluble Aβ42 fraction of the cortex, d) Soluble Aβ42 fraction of the hippocampus. (n=4 per group)

To evaluate the B9 distribuition after injection with the vectors ssAAV-CBA-B9-WPRE and scAAV-CBA-B9, brain sections were stained against the c-myc tag to compare the B9 distribution in hippocampus and cortex when a ssAAV vector or a scAAV vector was used (Fig. 7). The expression of B9 in the sections of mice injected with the ssAAV vector was widespread (Fig. 7a). Unexpectedly, in the sections taken from mice injected with the scAAV vector, B9 expression was limited to the hippocampus (Fig. 7b).

Furthermore, we performed a LC-MS/MS shotgun analysis of the proteome on samples from the cortex, to assess the relative amounts of B9 expression between mice injected with scAAV-CBA-

B9 and those injected with ssAAV-CBA-B9-WPRE. To establish which proteins were upregulated or downregulated, C57Bl/6 non-injected mice were used as a control. This approach allows a relative quantification and identification of proteins present in the sample, quantifying the fold-change between different conditions.

Mice injected with scAAV-CBA-B9 were expected to have a higher expression of the nanobody compared to those injected with ssAAV-CBA-B9-WPRE. Even though the nanobody was detected in the samples obtained from mice injected with scAAV-CBA-B9, there was no overexpression of B9 detected (Fig. 8a), which corroborates the results of the staining experiments. In the samples from mice injected with ssAAV-CBA-B9-WPRE there was a statistically significant overexpression of the nanobody, compared to controls (Fig. 8b), as well as in comparison to samples from mice injected with scAAV-CBA-B9 (Fig. 8c).

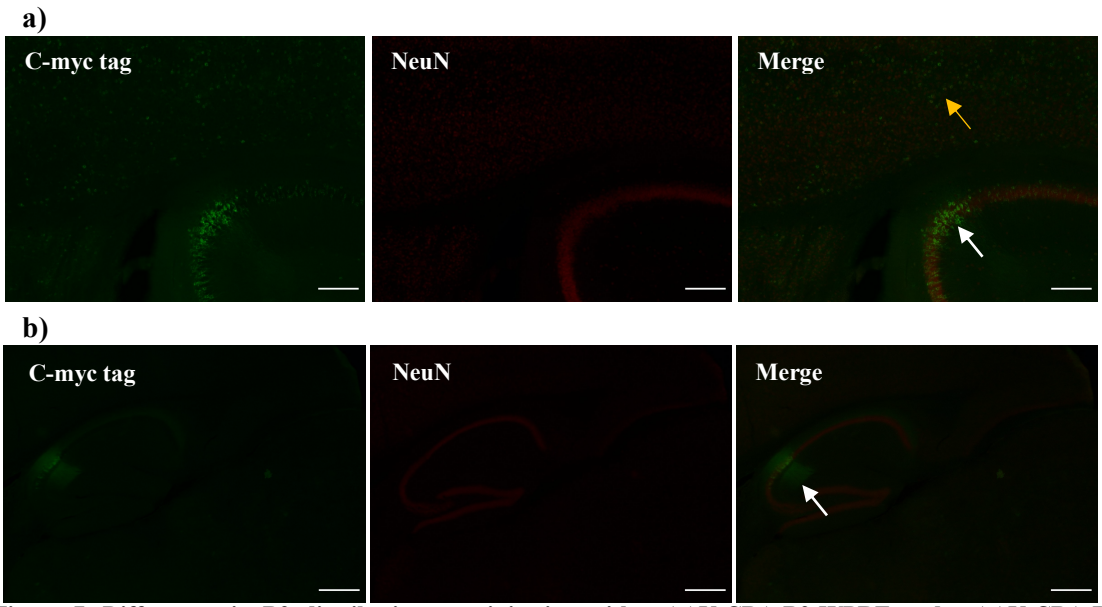

Figure 7. Differences in B9 distribution post-injection with ssAAV-CBA-B9-WPRE and scAAV-CBA-B9. Costaining of specific marker for neurons (NeuN, magenta) and marker for B9 (c-myc-tag, green). White arrows indicate B9 distribution on hippocampus region; yellow arrows indicate B9 distribution on cortex. a) Representative images from cortex and hippocampus regions systemically injected with ssAAV-CBA-B9-WPRE, objective APO5x. Scale bar: 50μm. b) Representative images from cortex and hippocampus regions systemically injected with scAAV-CBA-B9, objective APO2.5x. Scale bar: 100μm.

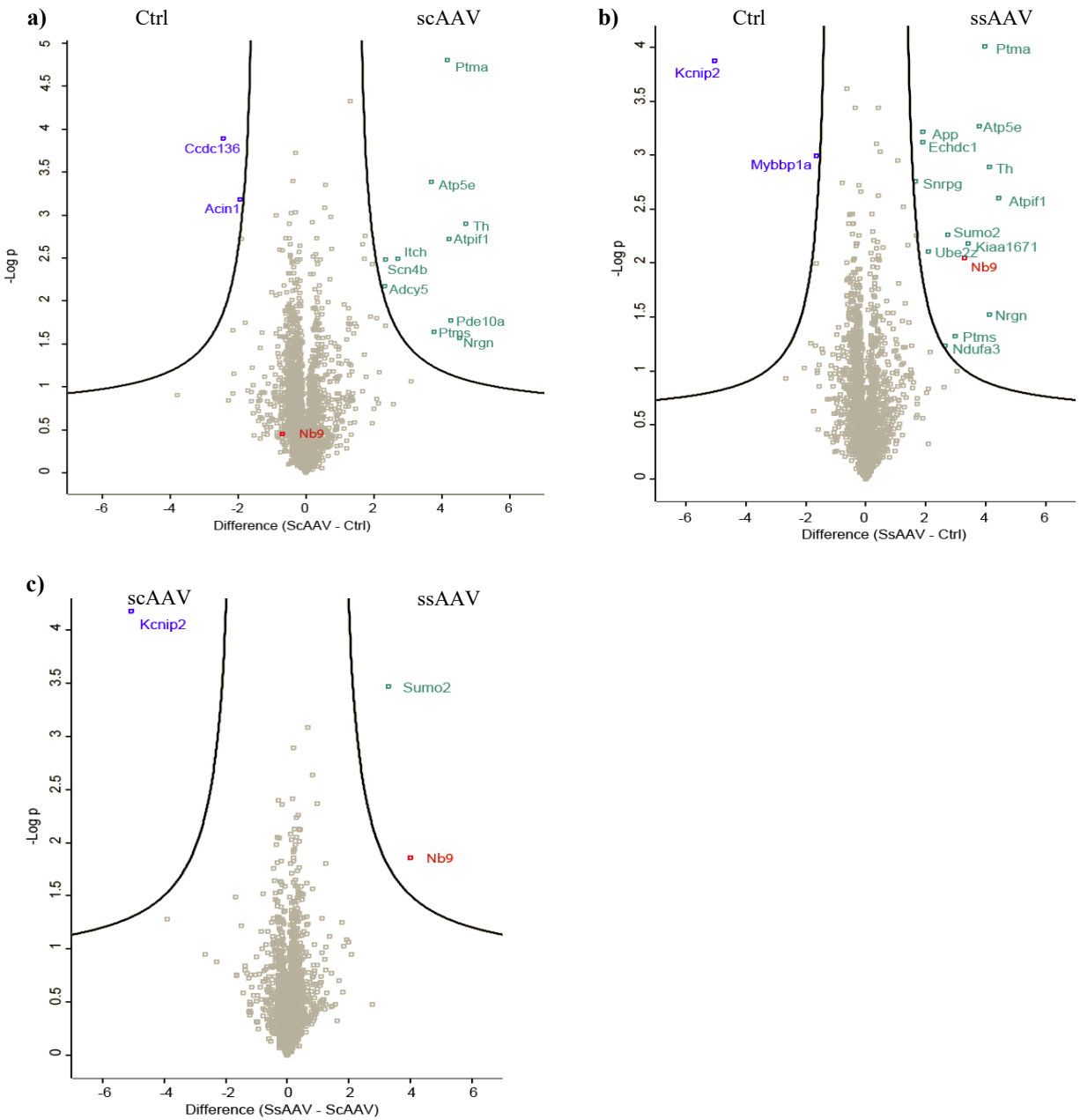

Figure 8. B9 is overexpressed only in the ssAAV-CBA-B9-WPRE injected mice. Volcano plot of shotgun proteomics: a) scAAV-CBA-B9 and C57Bl/6 samples pairwise comparison, b) ssAV-CBA-B9-WPRE and C57Bl/6 samples pairwise comparison , c) ssAAV-CBA-B9-WPRE and scAAV-CBA-B9 samples pairwise comparison. FDR = 0.05, $S_0 = 1$

5 Discussion

In gene therapy for CNS disorders, the delivery and expression of the transgene are the main concerns in the field (Deverman *et al*., 2016). In AD specifically, the main concern is the production of an efficient therapeutic molecule that halts the progression of the disease (Peng *et al.,* 2016; Heppner *et al*, 2015). AAV-based therapy emerges as an interesting mechanism to deliver the therapeutic a transgene, for instances encoding a potent nanobody with an anti-BACE1 activity, which is a promising novel therapy.

The anti-BACE1 activity of the nanobody B9 was previously validated *in vitro* (Rincon *et al*., unpublished). The administration of the nanobody decreased the activity of BACE1 without affecting the protein levels, however changes in Aβ levels were observed (US8568717B2, https://patents.google.com/patent/US8568717B2/en). In order to validate the activity of the nanobody *in vivo*, the Aβ species were measured. Despite not being a direct quantification of the nanobody, it is possible to extrapolate the anti-BACE1 activity of the nanobody, since there are changes in the Aβ content between the control injected group and the group injected with the vector containing the nanobody. The main focus of the measurements of Aβ40 and Aβ42 was the insoluble fraction since it has an important role in the onset of the disease (Wang *et al.,* 1999), therefore major changes in these fractions are relevant for validation and efficiency of the therapy. Moreover, the Aβ42 fractions were also considered relevant to the AD model strains, since this peptide is more prone to aggregate and form the amyloid plaques, an hallmark of AD (Jankowsky and Zheng, 2017).

The efficiency of B9 in decreasing Aβ species was tested in multiple strains, since the therapeutic response may vary between them. APP^{Dutch} strain is characterized for the high ratio of Aβ40/42, and accumulates Aβ principally around the cerebral vasculature (Herzig *et al.*, 2004). Parenchymal amyloid plaques, typical of AD in patients, are not observed. Therefore, we measured the changes of Aβ content post-injection with the vector bearing the nanobody in two alternative AD models, $APP^{NL\text{-}G\text{-}F}$ and APP/PS1, which both show deposition of parenchymal plaques.

The decrease of Aβ species in APP^{Dutch} mice and $APP^{NL\text{-}G\text{-}F}$ mice allowed the conclusion that B9 has anti-BACE1 activity *in vivo*, even though in APP/PS1 the results did not show any statistically significant decrease of Aβ peptides. This is possibly due to the severity of the model and rapid accumulation of Aβ (Radde *et al.,* 2006). However, validation of B9 activity in this murine model, if possible, would open the door for behavior tests, which would demonstrate a link between decreased Aβ load and improved cognition.

In order to validate B9 in APP/PS1, an optimized therapeutic window must be determined which allows changes in Aβ levels to be measured post vector administration. There is a clear age-dependent factor in the activity of B9, which could be related to the severity of the amyloidosis in each model (Radde *et al.,* 2006). The generation of Aβ peptides follows a sigmoid curve, if the B9 is administered when the levels of Aβ are in the exponential phase, it is easier to measure the difference in the levels of production than when the system is already in the plateau phase and saturated of Aβ species (Kumar and Walter, 2011), Therefore, the decrease of the peptide is not measurable, and the therapeutic effect of the nanobody is neglectable. An alternative to this approach is to boost the expression of the nanobody, it was expected that a higher expression of the nanobody to have an increase the impact on the levels of Aβ species.

To test if a scAAV without the regulatory elements would actually boost the expression of B9, a scAAV-CBA-B9 vector was produced and injected in the already validated APP^{Dutch} mice. As a control, the ssAAV-CBA-B9-WPRE was used, thus comparing this conformation and the scAAV-CBA-B9. The scAAV conformation is reported to increase the transgene expression and to have a "ready-to" transcribe conformation, compared to the ssAAV (Rincon *et al*., 2018). The major drawback of the scAAV vector is the packaging capacity, compromising about half of the transgene size compared to ssAAV conformation (McCarty *et al.*, 2008). Therefore, in the scAAV-CBA-B9, the WPRE had to be removed, although the WPRE was reported to have a role in stabilizing the mRNA, allowing more efficient transgene expression (Sun *et al.*, 2009; Wang *et al.*, 2016). In mice injected with the scAAV vector, we expected B9 expression would be higher, and consequently changes in Aβ levels would be more pronounced, when compared to mice injected with ssAAV. However, the Aβ content measured was equivalent in both groups. However, it should be noted that there was also no change in the Aβ content between control and B9 injected mice, which may be related to the fact that very young mice were used, in which amyloid levels were much lower than usually assayed. Furthermore, we assessed the impact of genome configuration on nanobody expression using LC-MS/MS, in which samples from mice injected with ssAAV-CBA-B9-WPRE showed higher B9 expression compared with those injected with scAAV-CBA-B9, corroborating the results from our immunohistochemistry experiments. Therefore, we concluded that even though the scAAV conformation could potencially provide a boost in transgene expression, the whole ssAAV trangene cassette proved to be more efficient in the expression of the B9, showing the importance of the regulatory elements in the expression of a transgene.

In follow up experiments, in order to have a more accurate comparison for the efficiency between the ssAAV conformation and the scAAV conformation, a group has to be added, a ssAAV-CBA-B9 without the WPRE, to put in evidence the role of WPRE in the efficiency of the delivery of the vector, and expression of the transgene. Due to time constraints and lack of mice to fulfill a group, we were unable to implement a group of mice injected with the vector. Therefore, to progress with the experiment it is required that a group of mice at the already validated age of injection/analysis is injected with the previously injected vectors and ssAAV-CBA-B9 without the WPRE.

Nevertheless, this novel AAV-based nanobody delivery platform shows promise for the treatment of AD. Further improvements to the system, such as boosting transgene expression, and may lead to a more pronounced therapeutic effect. Finally, the base technology can be expanded and used to target other proteins implicated in various CNS disorders, for which there are currently limited treatment options, promising a revolution in how we approach the treatment of these conditions.

6 Bibliography

Aiuti, A., Biasco, L., Scaramuzza, S., Ferrua, F., Cicalese, M.P., Baricordi, C., Dionisio, F., Calabria, A., Giannelli, S., Castiello, M.C., Bosticardo, M., Evangelio, C., Assanelli, A., Casiraghi, M., Di Nunzio, S., Callegaro, L., Benati, C., Rizzardi, P., Pellin, D., Di Serio, C., Schmidt, M., Von Kalle, C., Gardner, J., Mehta, N., Neduva, V., Dow, D.J., Galy, A., Miniero, R., Finocchi, A., Metin, A., Banerjee, P.P., Orange, J.S., Galimberti, S., Valsecchi, M.G., Biffi, A., Montini, E., Villa, A., Ciceri, F., Roncarolo, M.G., Naldini, L., 2013. Lentiviral hematopoietic stem cell gene therapy in patients with Wiskott-Aldrich syndrome. Science 341, 1233151.

Balazs, A.B., Bloom, J.D., Hong, C.M., Rao, D.S., Baltimore, D., 2013. Broad protection against influenza infection by vectored immunoprophylaxis in mice. Nat Biotechnol 31, 647–652.

Balazs, A.B., Chen, J., Hong, C.M., Rao, D.S., Yang, L., Baltimore, D., 2011. Antibody-based protection against HIV infection by vectored immunoprophylaxis. Nature 481, 81–84.

Bannas, P., Hambach, J., Koch-Nolte, F., 2017. Nanobodies and Nanobody-Based Human Heavy Chain Antibodies As Antitumor Therapeutics. Front Immunol 8.

Bateman, R.J., Xiong, C., Benzinger, T.L.S., Fagan, A.M., Goate, A., Fox, N.C., Marcus, D.S., Cairns, N.J., Xie, X., Blazey, T.M., Holtzman, D.M., Santacruz, A., Buckles, V., Oliver, A., Moulder, K., Aisen, P.S., Ghetti, B., Klunk, W.E., McDade, E., Martins, R.N., Masters, C.L., Mayeux, R., Ringman, J.M., Rossor, M.N., Schofield, P.R., Sperling, R.A., Salloway, S., Morris, J.C., Dominantly Inherited Alzheimer Network, 2012. Clinical and biomarker changes in dominantly inherited Alzheimer's disease. N. Engl. J. Med. 367, 795–804.

Barão, S., Moechars, D., Lichtenthaler, S.F., De Strooper, B., 2016. BACE1 Physiological Functions May Limit Its Use as Therapeutic Target for Alzheimer's Disease. Trends in Neurosciences 39, 158–169.

Bouard, D., Alazard-Dany, D., Cosset, F.-L., 2009. Viral vectors: from virology to transgene expression. Br. J. Pharmacol. 157, 153–165.

Bourdenx, M., Dutheil, N., Bezard, E., Dehay, B., 2014. Systemic gene delivery to the central nervous system using Adeno-associated virus. Front. Mol. Neurosci. 7.

Braak, H., Braak, E., 1991. Demonstration of Amyloid Deposits and Neurofibrillary Changes in Whole Brain Sections. Brain Pathology.

Chávez-Gutiérrez, L., Bammens, L., Benilova, I., Vandersteen, A., Benurwar, M., Borgers, M., Lismont, S., Zhou, L., Van Cleynenbreugel, S., Esselmann, H., Wiltfang, J., Serneels, L., Karran, E., Gijsen, H., Schymkowitz, J., Rousseau, F., Broersen, K., De Strooper, B., 2012. The mechanism of γ-Secretase dysfunction in familial Alzheimer disease. EMBO J. 31, 2261–2274.

Choudhury, S.R., Hudry, E., Maguire, C.A., Sena-Esteves, M., Breakefield, X.O., Grandi, P., 2017. Viral vectors for therapy of neurologic diseases. Neuropharmacology 120, 63–80.

Cox, D.B.T., Platt, R.J., Zhang, F., 2015. Therapeutic genome editing: prospects and challenges. Nature Medicine 21, 121–131.

Crystal, R.G., 2014. Adenovirus: The First Effective In Vivo Gene Delivery Vector. Hum Gene Ther 25, 3–11.

Cupers, P., Orlans, I., Craessaerts, K., Annaert, W., Strooper, B.D., 2001. The amyloid precursor protein (APP)-cytoplasmic fragment generated by γ-secretase is rapidly degraded but distributes partially in a nuclear fraction of neurones in culture. Journal of Neurochemistry 78, 1168–1178.

Deal, C.E., Balazs, A.B., 2015. Vectored Antibody Gene Delivery for the Prevention or Treatment of HIV Infection. Curr Opin HIV AIDS 10, 190–197.

De Strooper, B., Karran, E., 2016. The Cellular Phase of Alzheimer's Disease. Cell 164, 603–615.

Deverman, B.E., Pravdo, P.L., Simpson, B.P., Kumar, S.R., Chan, K.Y., Banerjee, A., Wu, W.-L., Yang, B., Huber, N., Pasca, S.P., Gradinaru, V., 2016. Cre-dependent selection yields AAV variants for widespread gene transfer to the adult brain. Nature Biotechnology 34, 204–209.

Dodiya, H.B., Bjorklund, T., Stansell, J., Mandel, R.J., Kirik, D., Kordower, J.H., 2010. Differential transduction following basal ganglia administration of distinct pseudotyped AAV capsid serotypes in nonhuman primates. Mol. Ther. 18, 579–587.

Dominguez, D., Tournoy, J., Hartmann, D., Huth, T., Cryns, K., Deforce, S., Serneels, L., Camacho, I.E., Marjaux, E., Craessaerts, K., Roebroek, A.J.M., Schwake, M., D'Hooge, R., Bach, P., Kalinke, U., Moechars, D., Alzheimer, C., Reiss, K., Saftig, P., De Strooper, B., 2005. Phenotypic and biochemical analyses of BACE1- and BACE2-deficient mice. J. Biol. Chem. 280, 30797–30806.

Escors, D., Breckpot, K., 2010. Lentiviral vectors in gene therapy: their current status and future potential. Arch Immunol Ther Exp (Warsz) 58, 107–119.

Ferreira-Vieira, T.H., Guimaraes, I.M., Silva, F.R., Ribeiro, F.M., 2016. Alzheimer's disease: Targeting the Cholinergic System. Curr Neuropharmacol 14, 101–115.

Flotte, T.R., 2004. Gene therapy progress and prospects: recombinant adeno-associated virus (rAAV) vectors. Gene Ther. 11, 805–810.

Foldvari, M., Chen, D.W., Nafissi, N., Calderon, D., Narsineni, L., Rafiee, A., 2016. Non-viral gene therapy: Gains and challenges of non-invasive administration methods. Journal of Controlled Release 240, 165–190.

Freskgård, P.-O., Urich, E., 2017. Antibody therapies in CNS diseases. Neuropharmacology 120, 38–55.

Gaspar, H.B., Cooray, S., Gilmour, K.C., Parsley, K.L., Adams, S., Howe, S.J., Al Ghonaium, A., Bayford, J., Brown, L., Davies, E.G., Kinnon, C., Thrasher, A.J., 2011. Long-term

persistence of a polyclonal T cell repertoire after gene therapy for X-linked severe combined immunodeficiency. Sci Transl Med 3, 97ra79.

Hassanzadeh-Ghassabeh, G., Devoogdt, N., De Pauw, P., Vincke, C., Muyldermans, S., 2013. Nanobodies and their potential applications. Nanomedicine 8, 1013–1026.

Hawkes, N., 2017. Merck ends trial of potential Alzheimer's drug verubecestat. BMJ 356, j845.

Heneka, M.T., Carson, M.J., Khoury, J.E., Landreth, G.E., Brosseron, F., Feinstein, D.L., Jacobs, A.H., Wyss-Coray, T., Vitorica, J., Ransohoff, R.M., Herrup, K., Frautschy, S.A., Finsen, B., Brown, G.C., Verkhratsky, A., Yamanaka, K., Koistinaho, J., Latz, E., Halle, A., Petzold, G.C., Town, T., Morgan, D., Shinohara, M.L., Perry, V.H., Holmes, C., Bazan, N.G., Brooks, D.J., Hunot, S., Joseph, B., Deigendesch, N., Garaschuk, O., Boddeke, E., Dinarello, C.A., Breitner, J.C., Cole, G.M., Golenbock, D.T., Kummer, M.P., 2015. Neuroinflammation in Alzheimer's disease. The Lancet Neurology 14, 388–405.

Heppner, F.L., Ransohoff, R.M., Becher, B., 2015. Immune attack: the role of inflammation in Alzheimer disease. Nature Reviews Neuroscience 16, 358–372.

Herzig, M.C., Winkler, D.T., Burgermeister, P., Pfeifer, M., Kohler, E., Schmidt, S.D., Danner, S., Abramowski, D., Stürchler-Pierrat, C., Bürki, K., van Duinen, S.G., Maat-Schieman, M.L.C., Staufenbiel, M., Mathews, P.M., Jucker, M., 2004. Abeta is targeted to the vasculature in a mouse model of hereditary cerebral hemorrhage with amyloidosis. Nat. Neurosci. 7, 954–960.

Hippius, H., Neundörfer, G., 2003. The discovery of Alzheimer's disease. Dialogues Clin Neurosci 5, 101–108.

Howe, S.J., Mansour, M.R., Schwarzwaelder, K., Bartholomae, C., Hubank, M., Kempski, H., Brugman, M.H., Pike-Overzet, K., Chatters, S.J., de Ridder, D., Gilmour, K.C., Adams, S., Thornhill, S.I., Parsley, K.L., Staal, F.J.T., Gale, R.E., Linch, D.C., Bayford, J., Brown, L., Quaye, M., Kinnon, C., Ancliff, P., Webb, D.K., Schmidt, M., von Kalle, C., Gaspar, H.B., Thrasher, A.J., 2008. Insertional mutagenesis combined with acquired somatic mutations causes leukemogenesis following gene therapy of SCID-X1 patients. J. Clin. Invest. 118, 3143–3150.

Hyman, B.T., Phelps, C.H., Beach, T.G., Bigio, E.H., Cairns, N.J., Carrillo, M.C., Dickson, D.W., Duyckaerts, C., Frosch, M.P., Masliah, E., Mirra, S.S., Nelson, P.T., Schneider, J.A., Thal, D.R., Thies, B., Trojanowski, J.Q., Vinters, H.V., Montine, T.J., 2012. National Institute on Aging-Alzheimer's Association guidelines for the neuropathologic assessment of Alzheimer's disease. Alzheimers Dement 8, 1–13.

Jankowsky, J.L., Zheng, H., 2017. Practical considerations for choosing a mouse model of Alzheimer's disease. Molecular Neurodegeneration 12.

Jarvik, L., Greenson, H., 1987. About a peculiar disease of the cerebral cortex. By Alois Alzheimer, 1907 (Translated by L. Jarvik and H. Greenson). Alzheimer Dis Assoc Disord 1, 3-8.

Jayant, R.D., Nair, M.G., 2016. Nanotechnology for the Treatment of NeuroAIDS.

Jayant, R.D., Sosa, D., Kaushik, A., Atluri, V., Vashist, A., Tomitaka, A., Nair, M., 2016. Current status of non-viral gene therapy for CNS disorders. Expert Opinion on Drug Delivery 13, 1433–1445.

Jonquieres, G. von, Mersmann, N., Klugmann, C.B., Harasta, A.E., Lutz, B., Teahan, O., Housley, G.D., Fröhlich, D., Krämer-Albers, E.-M., Klugmann, M., 2013. Glial Promoter Selectivity following AAV-Delivery to the Immature Brain. PLOS ONE 8, e65646.

Jooss, K., Chirmule, N., 2003. Immunity to adenovirus and adeno-associated viral vectors: implications for gene therapy. Gene Ther. 10, 955–963.

Jordão, J.F., Ayala-Grosso, C.A., Markham, K., Huang, Y., Chopra, R., McLaurin, J., Hynynen, K., Aubert, I., 2010. Antibodies targeted to the brain with image-guided focused ultrasound reduces amyloid-beta plaque load in the TgCRND8 mouse model of Alzheimer's disease. PLoS ONE 5, e10549.

Karran, E., Mercken, M., Strooper, B.D., 2011. The amyloid cascade hypothesis for Alzheimer's disease: an appraisal for the development of therapeutics. Nature Reviews Drug Discovery 10, 698–712.

Kay, M.A., 2011. State-of-the-art gene-based therapies: the road ahead. Nature Reviews Genetics 12, 316–328.

Kempuraj, D., Thangavel, R., Natteru, P., Selvakumar, G., Saeed, D., Zahoor, H., Zaheer, S., Iyer, S., Zaheer, A., 2017. Neuroinflammation Induces Neurodegeneration 15.

Kerem, B., Rommens, J.M., Buchanan, J.A., Markiewicz, D., Cox, T.K., Chakravarti, A., Buchwald, M., Tsui, L.C., 1989. Identification of the cystic fibrosis gene: genetic analysis. Science 245, 1073–1080.

Kimberly, W.T., Zheng, J.B., Guénette, S.Y., Selkoe, D.J., 2001. The intracellular domain of the beta-amyloid precursor protein is stabilized by Fe65 and translocates to the nucleus in a notch-like manner. J. Biol. Chem. 276, 40288–40292.

Kotterman, M.A., Chalberg, T.W., Schaffer, D.V., 2015. Viral Vectors for Gene Therapy: Translational and Clinical Outlook. Annual Review of Biomedical Engineering 17, 63–89.

Kumar, A., Singh, A., Ekavali, 2015. A review on Alzheimer's disease pathophysiology and its management: an update. Pharmacological Reports 67, 195–203.

Kumar, S., Walter, J., 2011. Phosphorylation of amyloid beta (Aβ) peptides – A trigger for formation of toxic aggregates in Alzheimer's disease. Aging (Albany NY) 3, 803–812.

Lahiri, D.K., Sambamurti, K., Bennett, D.A., 2004. Apolipoprotein gene and its interaction with the environmentally driven risk factors: molecular, genetic and epidemiological studies of

Alzheimer's disease. Neurobiology of Aging, Challenging Views of Alzheimer's Disease - Round II 25, 651–660.

Latif-Hernandez, A., Shah, D., Craessaerts, K., Saido, T., Saito, T., De Strooper, B., Van der Linden, A., D'Hooge, R., 2019. Subtle behavioral changes and increased prefrontal-hippocampal network synchronicity in APPNL−G−F mice before prominent plaque deposition. Behavioural Brain Research 364, 431–441.

Lewerenz, J., Maher, P., 2015. Chronic Glutamate Toxicity in Neurodegenerative Diseases-What is the Evidence? Front Neurosci 9, 469.

Lowry, O.H., Rosebrough, N.J., Farr, A.L., Randall, R.J., 1951. Protein measurement with the Folin phenol reagent. J. Biol. Chem. 193, 265–275.

Luo, Y., Bolon, B., Kahn, S., Bennett, B.D., Babu-Khan, S., Denis, P., Fan, W., Kha, H., Zhang, J., Gong, Y., Martin, L., Louis, J.C., Yan, Q., Richards, W.G., Citron, M., Vassar, R., 2001. Mice deficient in BACE1, the Alzheimer's beta-secretase, have normal phenotype and abolished beta-amyloid generation. Nat. Neurosci. 4, 231–232.

Lykken, E.A., Shyng, C., Edwards, R.J., Rozenberg, A., Gray, S.J., 2018. Recent progress and considerations for AAV gene therapies targeting the central nervous system. Journal of Neurodevelopmental Disorders 10.

MacDonald, M.E., Ambrose, C.M., Duyao, M.P., Myers, R.H., Lin, C., Srinidhi, L., Barnes, G., Taylor, S.A., James, M., Groot, N., MacFarlane, H., Jenkins, B., Anderson, M.A., Wexler, N.S., Gusella, J.F., Bates, G.P., Baxendale, S., Hummerich, H., Kirby, S., North, M., Youngman, S., Mott, R., Zehetner, G., Sedlacek, Z., Poustka, A., Frischauf, A.-M., Lehrach, H., Buckler, A.J., Church, D., Doucette-Stamm, L., O'Donovan, M.C., Riba-Ramirez, L., Shah, M., Stanton, V.P., Strobel, S.A., Draths, K.M., Wales, J.L., Dervan, P., Housman, D.E., Altherr, M., Shiang, R., Thompson, L., Fielder, T., Wasmuth, J.J., Tagle, D., Valdes, J., Elmer, L., Allard, M., Castilla, L., Swaroop, M., Blanchard, K., Collins, F.S., Snell, R., Holloway, T., Gillespie, K., Datson, N., Shaw, D., Harper, P.S., 1993. A novel gene containing a trinucleotide repeat that is expanded and unstable on Huntington's disease chromosomes. Cell 72, 971–983.

McCarty, D.M., 2008. Self-complementary AAV Vectors; Advances and Applications. Molecular Therapy 16, 1648–1656.

Misra, A., Ganesh, S., Shahiwala, A., Shah, S.P., 2003. Drug delivery to the central nervous system: a review. J Pharm Pharm Sci 6, 252–273.

Mockett, B.G., Richter, M., Abraham, W.C., Müller, U.C., 2017. Therapeutic Potential of Secreted Amyloid Precursor Protein APPsα. Front Mol Neurosci 10, 30.

Müller, U.C., Deller, T., Korte, M., 2017. Not just amyloid: physiological functions of the amyloid precursor protein family. Nat. Rev. Neurosci. 18, 281–298.

Naldini, L., 2015. Gene therapy returns to centre stage. Nature 526, 351–360.

Naso, M.F., Tomkowicz, B., Perry, W.L., Strohl, W.R., 2017. Adeno-Associated Virus (AAV) as a Vector for Gene Therapy. BioDrugs 31, 317–334.

Niewoehner, J., Bohrmann, B., Collin, L., Urich, E., Sade, H., Maier, P., Rueger, P., Stracke, J.O., Lau, W., Tissot, A.C., Loetscher, H., Ghosh, A., Freskgård, P.-O., 2014. Increased brain penetration and potency of a therapeutic antibody using a monovalent molecular shuttle. Neuron 81, 49–60.

Omerovic, M., Hampel, H., Teipel, S.J., Buerger, K., 2008. Pharmacological treatment of Alzheimer's dementia: state of the art and current dilemmas. World J. Biol. Psychiatry 9, 69–75.

Panza, F., Solfrizzi, V., Imbimbo, B.P., Logroscino, G., 2014. Amyloid-directed monoclonal antibodies for the treatment of Alzheimer's disease: the point of no return? Expert Opin Biol Ther 14, 1465–1476.

Peng, W., Achariyar, T.M., Li, B., Liao, Y., Mestre, H., Hitomi, E., Regan, S., Kasper, T., Peng, S., Ding, F., Benveniste, H., Nedergaard, M., Deane, R., 2016. Suppression of glymphatic fluid transport in a mouse model of Alzheimer's disease. Neurobiology of Disease 93, 215–225.

Peterson, L.R., Hall, W.H., Zinneman, H.H., Gerding, D.N., 1977. Standardization of a Preparative Ultracentrifuge Method for Quantitative Determination of Protein Binding of Seven Antibiotics. J Infect Dis 136, 778–783.

Picanco, L.C., Ozela, P.F., de Fatima de Brito Brito, M., Pinheiro, A.A., Padilha, E.C., Braga, F.S., de Paula da Silva, C.H.T., dos Santos, C.B.R., Rosa, J.M.C., da Silva Hage-Melim, L.I., 2018. Alzheimer's Disease: A Review from the Pathophysiology to Diagnosis, New Perspectives for Pharmacological Treatment

Portelius, E., Andreasson, U., Ringman, J.M., Buerger, K., Daborg, J., Buchhave, P., Hansson, O., Harmsen, A., Gustavsson, M.K., Hanse, E., Galasko, D., Hampel, H., Blennow, K., Zetterberg, H., 2010. Distinct cerebrospinal fluid amyloid beta peptide signatures in sporadic and PSEN1 A431E-associated familial Alzheimer's disease. Mol Neurodegener 5, 2.

Prince, M.J., 2016. World Alzheimer Report 2016 - Improving healthcare for people living with dementia: Coverage, quality and costs now and in the future https://www.alz.co.uk/research/world-report-2016 (accessed 8.12.19).

Prince, M.J., 2015. World Alzheimer Report 2015: The Global Impact of Dementia https://www.alz.co.uk/research/world-report-2015 (accessed 8.12.19).

Querfurth, H.W., LaFerla, F.M., 2010. Alzheimer's disease. N. Engl. J. Med. 362, 329–344.

Radde, R., Bolmont, T., Kaeser, S.A., Coomaraswamy, J., Lindau, D., Stoltze, L., Calhoun, M.E., Jäggi, F., Wolburg, H., Gengler, S., Haass, C., Ghetti, B., Czech, C., Hölscher, C., Mathews, P.M., Jucker, M., 2006. Abeta42-driven cerebral amyloidosis in transgenic mice reveals early and robust pathology. EMBO Rep. 7, 940–946.

Ramamoorth, M., Narvekar, A., 2015. Non Viral Vectors in Gene Therapy- An Overview. J Clin Diagn Res 9, GE01–GE06.

Read, J., Suphioglu, C., 2013. Dropping the BACE: Beta Secretase (BACE1) as an Alzheimer's Disease Intervention Target, in: Kishore, U. (Ed.), Neurodegenerative Diseases. InTech.

Rincon, M.Y., de Vin, F., Duqué, S.I., Fripont, S., Castaldo, S.A., Bouhuijzen-Wenger, J., Holt, M.G., 2018. Widespread transduction of astrocytes and neurons in the mouse central nervous system after systemic delivery of a self-complementary AAV-PHP.B vector. Gene Therapy 25, 83–92.

Rincon, M.Y., Zhou, L., Marneffe, C., Voytyuk, I., Wouters, Y., Dewilde, M., Duqué, S.I., Vincke, C., Levites, Y., Golde, T.E., Muyldermans, S., Strooper, B.D., Holt, M.G., unpublished. AAV mediated delivery of a novel anti-BACE1 VHH reduces Abeta in an Alzheimer's disease mouse model. bioRxiv 698506.

Riordan, J.R., Rommens, J.M., Kerem, B., Alon, N., Rozmahel, R., Grzelczak, Z., Zielenski, J., Lok, S., Plavsic, N., Chou, J.L., 1989. Identification of the cystic fibrosis gene: cloning and characterization of complementary DNA. Science 245, 1066–1073.

Robbins, P.D., Ghivizzani, S.C., 1998. Viral Vectors for Gene Therapy. Pharmacology & Therapeutics 80, 35–47.

Roberds, S.L., Anderson, J., Basi, G., Bienkowski, M.J., Branstetter, D.G., Chen, K.S., Freedman, S.B., Frigon, N.L., Games, D., Hu, K., Johnson-Wood, K., Kappenman, K.E., Kawabe, T.T., Kola, I., Kuehn, R., Lee, M., Liu, W., Motter, R., Nichols, N.F., Power, M., Robertson, D.W., Schenk, D., Schoor, M., Shopp, G.M., Shuck, M.E., Sinha, S., Svensson, K.A., Tatsuno, G., Tintrup, H., Wijsman, J., Wright, S., McConlogue, L., 2001. BACE knockout mice are healthy despite lacking the primary beta-secretase activity in brain: implications for Alzheimer's disease therapeutics. Hum. Mol. Genet. 10, 1317–1324.

Rochin, L., Hurbain, I., Serneels, L., Fort, C., Watt, B., Leblanc, P., Marks, M.S., De Strooper, B., Raposo, G., van Niel, G., 2013. BACE2 processes PMEL to form the melanosome amyloid matrix in pigment cells. Proc. Natl. Acad. Sci. U.S.A. 110, 10658–10663.

Rommens, J.M., Iannuzzi, M.C., Kerem, B., Drumm, M.L., Melmer, G., Dean, M., Rozmahel, R., Cole, J.L., Kennedy, D., Hidaka, N., 1989. Identification of the cystic fibrosis gene: chromosome walking and jumping. Science 245, 1059–1065.

Saito, T., Matsuba, Y., Mihira, N., Takano, J., Nilsson, P., Itohara, S., Iwata, N., Saido, T.C., 2014. Single App knock-in mouse models of Alzheimer's disease. Nat. Neurosci. 17, 661–663.

Saito, T., Saido, T.C., 2018. Neuroinflammation in mouse models of Alzheimer's disease. Clinical and Experimental Neuroimmunology 9, 211–218.

Saito, T., Suemoto, T., Brouwers, N., Sleegers, K., Funamoto, S., Mihira, N., Matsuba, Y., Yamada, K., Nilsson, P., Takano, J., Nishimura, M., Iwata, N., Van Broeckhoven, C., Ihara, Y.,

Saido, T.C., 2011. Potent amyloidogenicity and pathogenicity of Aβ43. Nature Neuroscience 14, 1023–1032.

Sakakibara, Y., Sekiya, M., Saito, T., Saido, T.C., Iijima, K.M., 2018. Cognitive and emotional alterations in App knock-in mouse models of Aβ amyloidosis. BMC Neuroscience 19.

Samulski, R.J., Muzyczka, N., 2014. AAV-Mediated Gene Therapy for Research and Therapeutic Purposes. Annu Rev Virol 1, 427–451.

Sanders, J.W., Ponzio, T.A., 2017. Vectored immunoprophylaxis: an emerging adjunct to traditional vaccination. Trop Dis Travel Med Vaccines 3.

Seabrook, G.R., Smith, D.W., Bowery, B.J., Easter, A., Reynolds, T., Fitzjohn, S.M., Morton, R.A., Zheng, H., Dawson, G.R., Sirinathsinghji, D.J., Davies, C.H., Collingridge, G.L., Hill, R.G., 1999. Mechanisms contributing to the deficits in hippocampal synaptic plasticity in mice lacking amyloid precursor protein. Neuropharmacology 38, 349–359.

Selkoe, D.J., Hardy, J., 2016. The amyloid hypothesis of Alzheimer's disease at 25 years. EMBO Mol Med 8, 595–608.

Serrano-Pozo, A., Frosch, M.P., Masliah, E., Hyman, B.T., 2011. Neuropathological alterations in Alzheimer disease. Cold Spring Harb Perspect Med 1, a006189.

Shimshek, D.R., Jacobson, L.H., Kolly, C., Zamurovic, N., Balavenkatraman, K.K., Morawiec, L., Kreutzer, R., Schelle, J., Jucker, M., Bertschi, B., Theil, D., Heier, A., Bigot, K., Beltz, K., Machauer, R., Brzak, I., Perrot, L., Neumann, U., 2016. Pharmacological BACE1 and BACE2 inhibition induces hair depigmentation by inhibiting PMEL17 processing in mice. Sci Rep 6, 21917.

Steeland, S., Vandenbroucke, R.E., Libert, C., 2016. Nanobodies as therapeutics: big opportunities for small antibodies. Drug Discov. Today 21, 1076–1113.

Sun, J., Li, D., Hao, Y., Zhang, Y., Fan, W., Fu, J., Hu, Y., Liu, Y., Shao, Y., 2009. Posttranscriptional Regulatory Elements Enhance Antigen Expression and DNA Vaccine Efficacy. DNA Cell Biol 28, 233–240.

Szaruga, M., Veugelen, S., Benurwar, M., Lismont, S., Sepulveda-Falla, D., Lleo, A., Ryan, N.S., Lashley, T., Fox, N.C., Murayama, S., Gijsen, H., Strooper, B.D., Chávez-Gutiérrez, L., 2015. Qualitative changes in human γ-secretase underlie familial Alzheimer's disease. Journal of Experimental Medicine 212, 2003–2013.

Terryn, S., Francart, A., Lamoral, S., Hultberg, A., Rommelaere, H., Wittelsberger, A., Callewaert, F., Stohr, T., Meerschaert, K., Ottevaere, I., Stortelers, C., Vanlandschoot, P., Kalai, M., Gucht, S.V., 2014. Protective Effect of Different Anti-Rabies Virus VHH Constructs against Rabies Disease in Mice. PLOS ONE 9, e109367.

Timbie, K.F., Mead, B.P., Price, R.J., 2015. Drug and gene delivery across the blood-brain barrier with focused ultrasound. J Control Release 219, 61–75.

Timmers, W.F., Tagliavini, F., Haan, J., Frangione, B., 1990. Parenchymal preamyloid and amyloid deposits in the brains of patients with hereditary cerebral hemorrhage with amyloidosis--Dutch type. Neurosci. Lett. 118, 223–226.

Upadhyay, R.K., 2014. Drug delivery systems, CNS protection, and the blood brain barrier. Biomed Res Int 2014, 869269.

Vaishnaw, A.K., Gollob, J., Gamba-Vitalo, C., Hutabarat, R., Sah, D., Meyers, R., de Fougerolles, T., Maraganore, J., 2010. A status report on RNAi therapeutics. Silence 1, 14.

Vassar, R., Kuhn, P.-H., Haass, C., Kennedy, M.E., Rajendran, L., Wong, P.C., Lichtenthaler, S.F., 2014. Function, therapeutic potential and cell biology of BACE proteases: current status and future prospects. J. Neurochem. 130, 4–28.

Veugelen, S., Saito, T., Saido, T.C., Chávez-Gutiérrez, L., De Strooper, B., 2016. Familial Alzheimer's Disease Mutations in Presenilin Generate Amyloidogenic Aβ Peptide Seeds. Neuron 90, 410–416.

Wagner, H., Wehrle, S., Weiss, E., Cavallari, M., Weber, W., 2018. A Two-Step Approach for the Design and Generation of Nanobodies. International Journal of Molecular Sciences 19, 3444.

Wang, B., Wang, Z., Sun, L., Yang, L., Li, H., Cole, A.L., Rodriguez-Rivera, J., Lu, H.-C., Zheng, H., 2014. The amyloid precursor protein controls adult hippocampal neurogenesis through GABAergic interneurons. J. Neurosci. 34, 13314–13325
.

Wang, J., Dickson, D.W., Trojanowski, J.Q., Lee, V.M.-Y., 1999. The Levels of Soluble versus Insoluble Brain Aβ Distinguish Alzheimer's Disease from Normal and Pathologic Aging. Experimental Neurology 158, 328–337.

Wang, L., Wang, Z., Zhang, F., Zhu, R., Bi, J., Wu, J., Zhang, H., Wu, H., Kong, W., Yu, B., Yu, X., 2016. Enhancing Transgene Expression from Recombinant AAV8 Vectors in Different Tissues Using Woodchuck Hepatitis Virus Post-Transcriptional Regulatory Element. Int J Med Sci 13, 286–291.

Wang, W., Liu, Y., Lazarus, R.A., 2013. Allosteric inhibition of BACE1 by an exosite-binding antibody. Curr. Opin. Struct. Biol. 23, 797–805.

Wisniewski, T., 2012. Active immunotherapy for Alzheimer's disease. Lancet Neurol 11, 571–572.

Yang, L., Wang, Z., Wang, B., Justice, N.J., Zheng, H., 2009. Amyloid precursor protein regulates Cav1.2 L-type calcium channel levels and function to influence GABAergic short-term plasticity. J. Neurosci. 29, 15660–15668.

Zafir-Lavie, I., Sherbo, S., Goltsman, H., Badinter, F., Yeini, E., Ofek, P., Miari, R., Tal, O., Liran, A., Shatil, T., Krispel, S., Shapir, N., Neil, G.A., Benhar, I., Panet, A., Satchi-Fainaro, R.,

2018. Successful intracranial delivery of trastuzumab by gene-therapy for treatment of HER2-positive breast cancer brain metastases. Journal of Controlled Release 291, 80–89.

Zhao, J., Deng, Y., Jiang, Z., Qing, H., 2016. G Protein-Coupled Receptors (GPCRs) in Alzheimer's Disease: A Focus on BACE1 Related GPCRs. Frontiers in Aging Neuroscience 8.

Zhou, L., Chávez-Gutiérrez, L., Bockstael, K., Sannerud, R., Annaert, W., May, P.C., Karran, E., Strooper, B.D., 2011. Inhibition of β-Secretase in Vivo via Antibody Binding to Unique Loops (D and F) of BACE1. J. Biol. Chem. 286, 8677–8687.